

AD-A037 524

CALIFORNIA UNIV LOS ANGELES DEPT OF PHYSICS

F/G 20/9

GENERATION OF DENSITY CAVITIES AND LOCALIZED ELECTRIC FIELDS IN--ETC(U)

N0001475-C-0476

JAN 77 S J MORALES, Y C LEE

NL

UNCLASSIFIED

PPG-292

1 OF 1
AD
A037524



END END

DATE FILMED 4-77 DATE FILMED 4-77

ADA037524

AD No.
DDC FILE COPY

REPORT DOCUMENTATION PAGE			READ INSTRUCTIONS BEFORE COMPLETING FORM
1. REPORT NUMBER <u>(24) PPG-292</u>	2. GOVT ACCESSION NO.	3. RECIPIENT'S CATALOG NUMBER <u>10</u>	
4. TITLE (and Subtitle) Generation of Density Cavities and Localized Electric Fields in a Nonuniform Plasma		5. TYPE OF REPORT & PERIOD COVERED <u>95</u> Technical <i>rept.</i>	
6. AUTHOR(s) <u>G. J. Morales and Y. C. Lee</u>		7. CONTRACT OR GRANT NUMBER(s) <u>ONR N0001475-C-0476-P00002</u>	
8. PERFORMING ORGANIZATION NAME AND ADDRESS Department of Physics University of California <i>univ</i> Los Angeles, California 90024		9. PROGRAM ELEMENT, PROJECT, TASK AREA & WORK UNIT NUMBERS <u>NR-012-306</u>	
10. CONTROLLING OFFICE NAME AND ADDRESS Office of Naval Research Physics Program Office Arlington, Virginia 22217		11. REPORT DATE <u>11 Jan 1977</u>	
12. MONITORING AGENCY NAME & ADDRESS (if different from Controlling Office)		13. NUMBER OF PAGES <u>58 pages</u>	
		14. SECURITY CLASS. (of this report) <u>Unclassified</u>	
		15. DECLASSIFICATION/DOWNGRADING SCHEDULE <u>Unclassified</u>	
16. DISTRIBUTION STATEMENT (of this Report) Approved for public release: distribution unlimited.			
17. DISTRIBUTION STATEMENT (of the abstract entered in Block 20, if different from Report)			
18. SUPPLEMENTARY NOTES To be published in <u>Physics of Fluids</u>			
19. KEY WORDS (Continue on reverse side if necessary and identify by block number) Localized fields, Cavitons, Lasar plasma attraction.			
20. ABSTRACT (Continue on reverse side if necessary and identify by block number) See attached sheet <i>next page</i>			

ABSTRACT

A simple model is presented which is capable of describing the detailed space-time evolution of the interaction of long wavelength electromagnetic radiation with an unmagnetized plasma having a nonuniform density profile. The model consists of describing the electric field via the nonlinear Schrodinger equation and the density changes through the ion-acoustic wave equation with the ponderomotive force effects included self-consistently. In the linear regime, this formulation explains the time evolution of the mode-conversion process that leads to the excitation of a short wavelength Langmuir wave in the neighborhood of the resonance layer where the frequency of the external radiation matches the local value of the electron plasma frequency. In the nonlinear regime, the model predicts the generation of density cavities and the associated spatial localization of the electric field. These features are in good agreement with the experimental results of Kim, Wong, and Stenzel. In addition, the model predicts a variety of new interesting phenomena such as the excitation of ion-acoustic oscillations and nonlinear relaxation oscillations which are amenable to experimental observation.

ACCESSION FOR	White Section	<input checked="" type="checkbox"/>
NTIS	Buff Section	<input type="checkbox"/>
DOC		<input type="checkbox"/>
UNANNOUNCED		
JUSTIFICATION		
BY		
DISTRIBUTION/AVAILABILITY CODES		
Dist.	Avail. Reg./or	SPECIAL
A		

**GENERATION OF DENSITY CAVITIES AND LOCALIZED
ELECTRIC FIELDS IN A NONUNIFORM PLASMA**

G. J. Morales and Y. C. Lee

PPG-292

January 1977

**Department of Physics
University of California
Los Angeles, California 90024**

ABSTRACT

A simple model is presented which is capable of describing the detailed space-time evolution of the interaction of long wavelength electromagnetic radiation with an unmagnetized plasma having a nonuniform density profile. The model consists of describing the electric field via the nonlinear Schrodinger equation and the density changes through the ion-acoustic wave equation with the ponderomotive force effects included self-consistently. In the linear regime, this formulation explains the time evolution of the mode-conversion process that leads to the excitation of a short wavelength Langmuir wave in the neighborhood of the resonance layer where the frequency of the external radiation matches the local value of the electron plasma frequency. In the nonlinear regime, the model predicts the generation of density cavities and the associated spatial localization of the electric field. These features are in good agreement with the experimental results of Kim, Wong, and Stenzel. In addition, the model predicts a variety of new interesting phenomena such as the excitation of ion-acoustic oscillations and nonlinear relaxation oscillations which are amenable to experimental observation.

I. INTRODUCTION

The interaction of intense electromagnetic radiation with plasmas is a subject of considerable interest because its study merges basic physics processes with a wealth of potential applications which may impact the development of future technologies. The basic physics aspects of this interaction are intimately connected with the behavior of strong plasma turbulence, i.e., that state of plasmas in which the zero-order properties of the medium (e.g., density, temperature, mean flow velocity) are modified to such a large extent that its description in terms of high-order perturbation theories based on the linear collective properties, are inapplicable.

The practical aspect of the interaction of intense electromagnetic radiation with plasmas is connected principally with its role as a method for increasing the plasma temperature. At the present time the two major applications of this role pertain to the RF heating of magnetically confined plasmas and to the laser-pellet fusion concept.

Another application, not necessarily technologically oriented, of the study of the interaction of intense radiation with plasmas pertains to the interpretation of the spontaneous radiation observed in space physics investigations. A better understanding of the basic nonlinear processes that play a role in this interaction may help to uncover the behavior of remote events which govern the evolution of naturally occurring plasmas.

The present investigation isolates a specific nonlinear process encountered in the interaction of intense radiation with a nonuniform plasma. Namely, the nonlinear modification of the density profile produced by the ponderomotive force associated with the high frequency electric fields in the plasma. Of course, other interesting and important effects take place in this interaction (e.g., plasma heating, enhanced transport, spontaneous magnetic

fields), however since the plasma dielectrics are sensitive in zeroth order to density changes, it follows that the major deviation from the linear behavior appears first through this effect. The other changes in the plasma can thus be considered as consequences of the nonlinear distortion of the profile and the associated spatial localization of the electric field.

In the present study we concentrate on the effects produced by a long wavelength pump field on a plasma slab whose unperturbed density increases linearly with position. The long wavelength restriction does not necessarily imply that the results obtained are inapplicable to the interaction of laser light with a plasma. The reason for the relevance of long wavelength pumps in this connection is that an electromagnetic wave which propagates at an angle θ relative to the density gradient is turned around at the point in the plasma where $\omega_{pe} = \omega \cos \theta$, in which ω_{pe} is the local electron plasma frequency, and ω is the frequency of the radiation. Beyond this point the radiation penetrates the plasma in the form of an evanescent electric field which encounters an electrostatic resonance^{1,2} at the point $\omega = \omega_{pe}$. Therefore, the long wavelength pump in the present study replaces the role of the evanescent radiation encountered in the more realistic situation.

It should also be mentioned that detailed experimental studies can be performed in the laboratory by utilizing as the external pump the quasi-electrostatic field (near field) generated by a large grid or capacitor plate immersed in a plasma, as demonstrated by the study³ of Kim, Wong, and Stenzel. Thus, the type of effects investigated here are amenable to direct experimental investigation.

The formulation presented in this manuscript consists of describing the evolution of the electric field through the nonlinear Schrodinger equation in which the density modification is obtained from the ion-acoustic wave equation

with the effects of the ponderomotive force included self-consistently. A limited version of this model has been previously published⁴ by the present authors, in which the ion-acoustic equation is replaced by a static ponderomotive force effect. The results obtained with the earlier model have been found to be in good agreement with the overall features observed in the experiment³ of Kim, Wong, and Stenzel. However, due to the nature of the earlier model a series of interesting effects associated with ion inertia can not be described. Thus, the present more general formulation complements the previous results by showing that the overall physics of the problem (i.e., the generation of density cavities and localized electric fields) is not affected by the inclusion of ion inertia, and that an additional level of structure is uncovered.

The principal new effects associated with the ion inertia are: a) the generation of density pulses and ion-acoustic type of oscillations up and down the density gradient, b) the splitting of large density cavities into smaller subcavities, and c) the appearance of significant relaxation oscillations near the resonant point. Some of these effects have been reported verbally⁵ by the authors earlier, and the motivation for their publication at this time is provided by a recent, and on-going experiment⁶ by Wong and Divirgilio in which a greater degree of experimental sensitivity permits their observation.

The manuscript is organized as follows: In Sec. II the formulation is presented, the relevant scaling introduced, and the general properties are discussed. Sec. III discusses briefly the numerical methods and boundary conditions used to investigate the model equations. In Sec. IV the linear and nonlinear results obtained are presented. Conclusions regarding the present results are considered in Sec. V.

II. FORMULATION

We consider an unmagnetized plasma slab whose zero order unperturbed density n_0 is nonuniform and has the functional form

$$n_0(x) = n_p(1 + \frac{x}{L}) \quad (1)$$

where, x is the spatial coordinate, L is the gradient scale length, and $n_0(x=0) = n_p$ represents the absolute value of the density at the resonant point, i.e., $\omega = \omega_p(x=0)$. One is interested in describing the space-time evolution of the total high frequency field E which is represented in the form

$$E = E(x, t)e^{-i\omega t} + c.c. \quad (2)$$

In Eq.(2) the complex amplitude E is assumed to vary on a time-scale slower than $2\pi/\omega$, i.e., $|\partial E / \partial t| \ll |E|/\omega$, and no assumption is made concerning its spatial dependence, which is to be determined from the model equations. It is understood in Eq.(2) that the electric field being considered points along the density gradient, since we restrict our treatment to one dimension for the sake of simplicity. In the absence of plasma $E(x, t)$ is strictly constant in space and time and its value is equal to E_0 , which we identify with the amplitude of the long-wavelength radiation or capacitor plate field.

Combining the continuity and force equations for the high-frequency response of the electron fluid yields the following equation for the high-frequency density fluctuations, n_H ,

$$\frac{\partial^2}{\partial t^2} n_H - 3\bar{v}_e^2 \frac{\partial^2}{\partial x^2} n_H - \frac{\partial}{\partial x} \left[\frac{e}{m} (n_0 + n_L) E \right] = 0 \quad (3)$$

where, n_L refers to the slowly varying density fluctuations which are to be determined self-consistently.

In Eq.(3) e and m refer to the electron charge and mass, respectively, and \bar{v}_e represents the thermal velocity of the electrons.

The high-frequency field is connected to the density fluctuations through Poisson's equation

$$\frac{\partial}{\partial x} \mathcal{E} = -4\pi e n_H - 4\pi \rho_0 \quad (4)$$

in which ρ_0 refers explicitly to the external charge oscillations responsible for the generation of the pump electric field. Physically, ρ_0 can be identified with the oscillating charge on the capacitor plates, which in an experiment are located some distance away from the resonance layer. With this physical insight into the nature of ρ_0 , it is useful to express Eq.(4) in the form

$$\frac{\partial}{\partial x} (\mathcal{E} - \mathcal{E}_0) = -4\pi e n_H \quad (5)$$

where \mathcal{E}_0 refers to the pump field in the absence of plasma.

Using Eq.(5) to eliminate n_H and inserting the result into Eq.(3) yields

$$\frac{\partial}{\partial x} \left(\frac{\partial^2}{\partial t^2} (\mathcal{E} - \mathcal{E}_0) - 3v_e^2 \frac{\partial^2}{\partial x^2} \right) + \frac{4\pi e^2}{m} (n_0 + n_L) = 0 \quad (6)$$

and since

$$\mathcal{E}_0 = E_0 e^{-i\omega t} + c.c. \quad (7)$$

Eq.(7) implies that

$$\frac{2i}{\omega} \frac{\partial}{\partial t} E + \frac{3v_e^2}{\omega^2} \frac{\partial^2}{\partial x^2} E + \left[1 - \frac{4\pi e^2}{m} [n_0(x) + n_L] \right] E = E_0 \quad (8)$$

In arriving at Eq.(8) the term $\partial^2 E / \partial t^2$ has been neglected, as is characteristic of a modulational representation. Furthermore, the arbitrary spatially independent function implicit in the form of Eq.(6) has been set equal to zero, as is appropriate to this problem. The correctness of this choice is made clear if we consider the linear steady-state response of a cold plasma ($v_e = 0$), as predicted by Eq.(8). In this limit Eq.(8) reads simply

$$\epsilon E = E_0 \quad (9)$$

which is the result expected from elementary electrostatics and where ϵ refers to the cold plasma dielectric. The addition of a non-zero function of time to Eq.(8) would thus lead to an additional incorrect contribution in Eq.(9).

The slow time-scale equation governing the evolution of n_L is obtained by adding the force equations for the electron and ion fluids, thus yielding

$$\frac{\partial}{\partial t} v_L \approx - \frac{m}{M} \frac{\partial}{\partial x} \left[\frac{v_H^2}{2} \right] - \frac{c_s^2}{n_0} \frac{\partial}{\partial x} n_L \quad (10)$$

in which v_L refers to the slowly changing fluid velocity, c_s is the ion-acoustic speed, M is the ion mass, and

$$\frac{v_H^2}{2} = \left(\frac{e}{m\omega} \right)^2 |E|^2 \quad (11)$$

As is customary in Eq.(10) the effect of the small low frequency electric field is neglected; as well as the explicit nonlinearities regarding the ion fluid.

Combining Eq.(10) with the continuity equation produces

$$\frac{\partial^2}{\partial t^2} n_L - c_s^2 \frac{\partial^2}{\partial x^2} n_L = \frac{m}{M} \frac{\partial}{\partial x} \left\{ n_0 \frac{\partial}{\partial x} \left[\left(\frac{e}{m\omega} \right)^2 |E|^2 \right] \right\} \quad (12)$$

in which we proceed to neglect the spatial variation of n_0 because in this problem one is interested in the changes occurring in the neighborhood of the resonance point, hence Eq.(12) becomes

$$\frac{\partial^2}{\partial t^2} n_L - c_s^2 \frac{\partial^2}{\partial x^2} n_L = c_s^2 \frac{\partial^2}{\partial x^2} \left[\frac{|E|^2}{4\pi n_0 T} \right] \quad (13)$$

which is the ion-acoustic wave equation in which the effect of the self-consistent ponderomotive force manifests itself as a source term. The quantity T appearing in Eq.(13) represents the plasma temperature.

Equations (8) and (13) constitute a pair of coupled partial differential equations in which the effects of plasma nonuniformity, external pumping, and nonlinear generation of density fluctuations are contained. It is useful in these equations to introduce the following nonuniform medium scaling

$$\begin{aligned} Z &= (k_D L)^{2/3} (x/L), \quad \tau = (k_D L)^{-2/3} (\omega t/2) \\ A &= (k_D L)^{-2/3} (E/E_0), \quad k_D^{-2} \equiv 3(\bar{v}_e/\omega)^2 \end{aligned} \quad (14)$$

and for generality a collisional damping rate ν is introduced which scales as

$$\Gamma = (k_D L)^{2/3} (\nu/\omega) \quad . \quad (15)$$

Using the scaled variables Eq. (8) takes the form

$$i \frac{\partial}{\partial \tau} A + \frac{\partial^2}{\partial Z^2} A - \left[Z - i\Gamma + (k_D L)^{2/3} \frac{n_L}{n_p} \right] A = 1 \quad (16)$$

and Eq. (13) becomes

$$v^2 \frac{\partial^2}{\partial \tau^2} \left(\frac{n_L}{n_p} \right) - \frac{\partial^2}{\partial Z^2} \left(\frac{n_L}{n_p} \right) = \frac{(k_D L)^{4/3} E_0^2}{4\pi n_p T} \frac{\partial^2}{\partial Z^2} |A|^2 \quad (17)$$

with

$$v^2 = (k_D L)^{-2/3} (M/m) \quad . \quad (18)$$

From Eqs. (16) and (17) it becomes evident that the degree of nonlinearity in this problem is measured by the lumped parameter

$$p = (k_D L)^2 (E_0^2 / 4\pi n_p T) \quad , \quad (19)$$

and, accordingly, the scaled density fluctuations N which produce a significant effect in the evolution of the system are given by

$$N = (k_D L)^{-4/3} (E_0^2 / 4\pi n_p T)^{-1} (n_L / n_p) \quad . \quad (20)$$

With these variables the mathematical representation of the model is contained in the pair of equations

$$i \frac{\partial}{\partial \tau} A + \frac{\partial^2}{\partial z^2} A - (z - i\Gamma + pN)A = 1 \quad (21)$$

$$v^2 \frac{\partial^2}{\partial \tau^2} N - \frac{\partial^2}{\partial z^2} N = \frac{\partial^2}{\partial z^2} |A|^2 \quad . \quad (22)$$

To obtain a better physical insight into the behavior of the system predicted from Eqs.(21) and (22) let us concentrate first on the purely linear response. For small amplitude pumps (i.e., $p \ll 1$) the behavior of the system is determined by the linear equation

$$i\frac{\partial}{\partial\tau}A + \frac{\partial^2}{\partial z^2}A - (z - i\Gamma)A = 1 \quad (23)$$

Hence, in a plasma where collisional effects are negligible the early time evolution of the electric field is approximately determined by

$$i\frac{\partial}{\partial\tau}A - zA \approx 1 \quad (24)$$

thus showing that initially the pump field drives a collection of uncoupled local oscillators. In particular, the oscillator at $z=0$ is driven at exact resonance, hence its amplitude is expected to grow linearly in time.

The second spatial derivative appearing in Eq.(23) arises due to the thermal motion of the electrons, and is found to play a crucial role in the physics of the problem. This term introduces a coupling between the independent local oscillators driven by the pump, thus producing a net convection of the electric field energy away from the resonance point in the direction of decreasing plasma density. As a consequence of this convection, the amplitude of the electric field does not grow without bound at $z=0$. Instead, it reaches a steady-state level determined by the group velocity of the Langmuir wave excited by the effective transmitter consisting of a layer of local oscillators in the neighborhood of the resonant point. The order of magnitude of this steady-state amplitude is automatically contained in the scaling presented in Eq.(14), namely

$$E = (k_D L)^{2/3} E_0 A(z, \tau) \quad (25)$$

and where the magnitude of A is of order unity, as is shown in the following.

In the linear regime the steady-state behavior of the system is determined from

$$\frac{d^2}{dz^2} A - (z - i\Gamma) A = 1 \quad (26)$$

whose general solution has the form

$$A = a A_i(\xi) + b B_i(\xi) - \pi G_i(\xi) \quad (27)$$

where $\xi = z - i\Gamma$, and A_i , and B_i are the well-known Airy functions defined in Ref.(7). In Eq.(27) a and b are constants to be determined, and G_i is the inhomogeneous solution of Eq.(26) given by

$$G_i(\xi) = \frac{1}{3} B_i(\xi) + \int_0^\xi dy [A_i(\xi)B_i(y) - A_i(y)B_i(\xi)] \quad (28)$$

whose asymptotic behavior is

$$G_i \sim (\pi \xi)^{-1} \quad \text{for } \operatorname{Re} \xi \gg 1 \quad (29)$$

$$G_i \sim \pi^{-1/2} \xi^{-1/4} \cos\left(\frac{2}{3}\xi^{3/2} + \frac{\pi}{4}\right) \quad \text{for } \operatorname{Re} \xi \ll -1$$

Since

$$B_i \sim \pi^{-1/2} \xi^{-1/4} \exp\left(\frac{2}{3}\xi^{3/2}\right) \quad (30)$$

for $\operatorname{Re} \xi \gg 1$, this implies that $b=0$ in Eq.(27). Furthermore, since in the region $\operatorname{Re} \xi \ll 1$ (i.e., down the density gradient)

$$A_i(\xi) \sim \pi^{-1/2} \xi^{-1/4} \sin\left(\frac{2}{3}\xi^{3/2} + \frac{\pi}{4}\right) \quad (31)$$

the outgoing-wave boundary condition requires that $a=i\pi$, thus yielding the solution

$$A(\xi) = -\pi[G_i(\xi) + iA_i(\xi)] \quad (32)$$

which represents the steady-state pattern of the linear mode-conversion process, whose time evolution is determined by Eq.(23) and is discussed in Sec. IV.

-13-

Turning our attention to the nonlinear response of the system, it is apparent that in general one must contend with two coupled partial differential equations which must be solved self-consistently. However, a further simplification of the present model is obtained if in Eq.(23) one neglects the effect of ion inertia, i.e., one drops the term $V^2(\partial^2N/\partial\tau^2)$. This procedure is appropriate if $V^2 \ll 1$ or if, locally, the group velocity of the high-frequency field is small compared to the ion-acoustic speed. Hence, the results obtained using such an oversimplification are most accurate in the neighborhood of the cold plasma resonance, and especially in the region $z>0$ since there the electric field is evanescent. Accordingly, the results obtained using this approximation are not expected to be accurate for $z \ll -1$, since in this region the group velocity of the excited Langmuir wave increases as it propagates down the density gradient. As is shown in Sec. IV, D., when this approximation is lifted the gross behavior of the system remains essentially unchanged. Of course, in the more realistic model one uncovers additional features associated with the excitation of ion-acoustic oscillations.

Proceeding to implement the simplification previously mentioned transforms Eq.(22) into

$$\frac{\partial^2}{\partial z^2} N = - \frac{\partial^2}{\partial z^2} |A|^2 \quad (33)$$

which yields the static ponderomotive force change in density $N = -|A|^2$. With this result Eq.(21) becomes

$$i\frac{\partial}{\partial\tau} A + \frac{\partial^2}{\partial z^2} A - (z - i\Gamma - p|A|^2)A = 0 \quad (34)$$

which is the driven nonlinear Schrodinger equation in a nonuniform plasma, considered previously by the present authors.

Eq.(34) is the nonlinear counterpart of Eq.(23), hence it describes the process of nonlinear mode-conversion whereby the pump field initially mode-converts into a Langmuir wave near the resonance point, and in this process

it alters the density profile in a self-consistent manner. Clearly if $p \ll 1$, but non-zero, the effect caused by the nonlinearity is rather weak, hence it can be described by perturbation theory.

The object of such a perturbation theory is to describe the distortion of the linear pattern given by Eq. (32). The steady-state perturbation procedure can be formulated by considering the equation

$$\frac{d^2}{d\xi^2} A - \xi A - 1 = - p |A|^2 A \quad (35)$$

in which the right-hand side is treated as a small quantity. Therefore, it is useful to express A in terms of the nonlinear integral equation

$$A(\xi) = W(\xi) + \pi p \left[A_1(\xi) \int_{-\infty}^{\xi} dy |A(y)|^2 A(y) B_+(y) - B_+(\xi) \int_{\infty}^{\xi} dy |A(y)|^2 A(y) A_1(y) \right] \quad (36)$$

where $W(\xi)$ represents the linear solution given by Eq. (32), and

$$B_+(\xi) = B_1(\xi) + iA_1(\xi) \quad (37)$$

describes the appropriate outgoing wave weight function.

The representation provided by Eq. (36) provides a natural expansion technique which is useful for small values of p . The iterative procedure suggested by Eq. (36) consists of generating a sequence of approximations that use the previous value of A to evaluate the integrals on the right-hand side of Eq. (36); the starting approximation being $A^0(\xi) = W(\xi)$. We have investigated this iterative scheme and have found that it converges rapidly for values of $p < 0.5$. The physical reason behind the mathematical convergence is that at these low levels of nonlinearity the profile changes consist mainly of a slight reduction in the gradient scale-length, hence the wavefunctions which solve the problem are not topologically different from the Airy-type solution given by Eq. (32). However, for values of $p > 0.8$ it is found that the iteration

procedure does not converge. The physical reason behind such a behavior is that at this larger level of nonlinearity density cavities or pockets begin to appear in the profile, hence the corresponding wavefunctions are closer to soliton-like structures than to the prediction of Eq.(32). In the neighborhood of $p \sim 0.8$ a variety of sophisticated techniques need to be used in order to extract convergent solutions out of Eq.(36).

The nature and consequences of the weakly nonlinear effects that can be extracted from perturbation theory are presented in Sec. IV, B., in which the full time evolution of Eq.(34) is investigated numerically. The reason for deferring such presentation is due to the fact that the solutions of the time dependent problem are found to approach asymptotically the iterative steady-state solutions obtained from Eq.(36).

Before proceeding to examine numerically the detailed properties of the models defined by Eqs.(21) and (22), and by Eq.(34), it is worthwhile to discuss some important conceptual features contained in them.

It should be realized that in the present formulation it is implicitly assumed that there exist external agents that continue to generate the linear density profile described by Eq.(1). The nonlinear modification of the profile produced by the ponderomotive force through Eq.(22) is a local effect which is assumed not to alter the external methods of plasma production. This description is most appropriate for laboratory experiments operating under CW conditions, such as those of Kim, Wong, and Stenzel, and of Wong and DiVergilio. Effects such as changes in the profile due to the indirect modification of the ambipolar potential, or of the bulk streaming velocity, as may be the case for blow-off plasmas in laser-pellet experiments, are not included.

The present model does not include kinetic effects associated with direct particle-field interactions. This restriction is appropriate for the

description of the zero-order nonlinear evolution. However, due to the fluid nature of the model, it is unable to deal with the interesting questions pertaining to the formation of high energy tails in the electron velocity distribution function, of ion acceleration, of magnetic field generation, as well as the feedback of these effects on the generation of localized electric fields. The investigation of such complicated features fall in the realm of particle simulation codes⁸.

Finally, it should be noted that the generation of density cavities and localized electric fields in a nonuniform plasma does not require the amplitude of the electric to be very large. The quantity whose value determines the threshold for this regime is the parameter $p = (\omega L / \bar{v}_e)^2 (E_0^2 / 12\pi n_p T)$, which can be quite large experimentally (of order 1 or larger) even for modest levels of E_0^2 .

With these features in mind we proceed to consider briefly the numerical scheme used in investigating the model equations.

III. NUMERICAL PROCEDURE

The numerical technique used to solve Eq. (21) consists of discretizing the space and time variables in steps Δz , and $\Delta \tau$, respectively. One then implements the time-averaged Crank-Nicholson procedure which yields the finite difference equation

$$\frac{1}{\Delta \tau} (A_j - A_{j-1}) + \frac{1}{2(\Delta z)^2} (A_{j+1} - 2A_j + A_{j-1}) + \frac{1}{2(\Delta z)^2} (A_{j+1} - 2A_j + A_{j-1}) \\ - \frac{1}{2} (\epsilon_j A_j + \epsilon_{j-1} A_{j-1}) = 1 \quad (38)$$

where A_j refers to the present value of A at the j spatial grid point, and A_{j-1} to the corresponding value at the previous time step. The complex dielectric is

$$\epsilon_j = z_j + pN_j - i\Gamma_j \quad (39)$$

and with an equivalent meaning for ϵ_{j-1} .

If the values of A_j , ϵ_j , and ϵ_{j-1} are known, Eq. (38) provides a matrix equation for the unknown A_j . The matrix equation can be solved in a quick and efficient manner through the tri-diagonal scheme,⁹ thus resulting in the implicit determination of the electric field amplitude at every time step.

To implement the tri-diagonal scheme requires a prior knowledge of N_j , since it appears explicitly in ϵ_j . For the model defined by Eq. (34), i.e., where ion-inertia is neglected, the required N_j at the present time τ is obtained through the extrapolation

$$N_j(\tau) = - [2|A_j(\tau-\Delta\tau)|^2 - |A_j(\tau-2\Delta\tau)|^2] \quad (40)$$

When dealing with the more general model defined by Eqs. (21) and (22), N_j is obtained by introducing an ion time step $\Delta\tau_i = \Delta\tau/V = \Delta z$ that permits the solution of Eq. (22) through the use of its characteristic mesh. To make the two time meshes coincide, a delay-time integer d is introduced, and the following algorithm is used to update N_j .

$$\begin{aligned} N_j(\tau) = & N_{j+1}(\tau-d\Delta\tau) + N_{j-1}(\tau-d\Delta\tau) - N_j(\tau-2d\Delta\tau) + |A_{j+1}(\tau-d\Delta\tau)|^2 - 2|A_j(\tau-d\Delta\tau)|^2 \\ & + |A_{j-1}(\tau-d\Delta\tau)|^2 \end{aligned} \quad (41)$$

The boundary conditions imposed on N_j when Eq.(22) is implemented consists simply of free propagation out of both ends of the finite plasma slab retained in the computer.

To handle the boundary conditions associated with the solution of Eq.(38) one uses a plasma slab whose width is large enough so that the important phenomena occurring near the resonant layer (i.e., $z=0$) does not sample the edges. Under such condition one updates the boundary values through the equation

$$i\frac{\partial}{\partial\tau} A - \epsilon A = 1 \quad (42)$$

which represents, physically, the cold plasma response. Eq.(42) is quite appropriate for describing the behavior of the plasma for $z \gg 1$ because the Langmuir waves are evanescent there. However, the application of Eq.(42) to the region $z \ll 1$ in the presence of mode-conversion is not quite consistent because Langmuir waves are continuously generated near $z=0$ and proceed to propagate down the density gradient. In an actual experiment the mode-converted waves experience strong Landau damping in the region $z \ll -1$ because their phase velocity decreases monotonically. However, in the present fluid description there are no mechanisms which prevent the mode-converted waves from reaching the boundary in the region $z \ll -1$, hence one must implement a numerical procedure which gives rise to a behavior consistent with the boundary equation. A simple scheme which overcomes this difficulty consists of introducing a damping coefficient $\Gamma(z)$ whose strength increases as one approaches the boundary. A typical choice used in the present investigation is

$$\Gamma(z) = \Gamma_0 + \Gamma_1 \exp\{-(z+20)^2/5\} \quad (43)$$

with $\Gamma_1 \sim 3-5$, and $\Gamma_0 = 0.2$. The choice of the constant damping Γ_0 used throughout this investigation is consistent with the conditions of the experiment of Kim, Wong, and Stenzel.

Another difficulty encountered in implementing the numerical solution of Eq.(38) via the tri-diagonal scheme is that for $z \ll -1$ the wavelength of the mode-converted wave decreases monotonically. When this physical behavior is translated to a finite mesh it can lead to spurious instabilities and reflections. This nuisance can be eliminated without altering the interesting physics near the resonance point by introducing a zero-order unperturbed profile which flattens as one approaches the low density boundary. A typical profile used in the present investigations is

$$\frac{n_0(z)}{n_p} = \begin{cases} -10 & \text{for } -20 \leq z \leq -15 \\ z+5 \exp[-(z+15)/5] & \text{for } -15 < z \end{cases} \quad (44)$$

which in conjunction with Eq.(43) provides a convenient way of modeling the absorption typically encountered in the laboratory in the low density region of the plasma.

Finally, it should be mentioned that the solution of Eqs.(21) and (22) is initialized with $N=0$, and through a sudden turn-on of the system.

In Sec. IV we proceed to discuss the linear and nonlinear results obtained by implementing this scheme in the mathematical on-line system at the University of California, Los Angeles.

IV. RESULTS

A. Linear Behavior

The linear response (i.e., $p=0$) of the system being considered consists of the mode-conversion process whereby the long wavelength radiation excites a Langmuir wave near $z=0$; the steady-state solution being given by Eq.(32). To obtain the time evolution of the events which lead to the formation of such a steady-state pattern one needs to solve Eq.(23) numerically. We proceed next to discuss the results of such a study.

In Fig. 1 we display the spatial dependence of $|A|^2$ for different times in the early evolution of the system, $0.5 < \tau < 1.5$. The sloping straight line represents the quantity $-\text{Re } \epsilon' = z$ which corresponds to the scaled real part of the dielectric, and thus to the scaled zero-order density profile. It is seen in Fig. 1 that the initial response corresponds to the excitation of the cold plasma resonance centered at $z=0$. It is found that the initial secular build-up of $|A|^2$ is suitably described by the approximate Eq.(42), in which the wave convection effects are neglected. The effect of convection is negligible at the early stage because the spatial curvature of A is not of much significance, since the external pump is spatially uniform. However, the purely cold plasma behavior does not last long. As soon as a significant curvature of A develops, the convection effects become important, as is shown in Fig. 2. This figure displays the spatial dependence of $|A|^2$ over the interval $2.0 < \tau < 3.0$, and demonstrates that wave convection stops the secular growth of the electric field and shifts the location of its peak toward the underdense side of the cold plasma resonance (i.e., toward $z < 0$). In addition, one observes that the electric field pattern begins to spread down the density gradient and that simultaneously interference oscillations in $|A|^2$ develop. These oscillations arise due to the interference between the mode-converted wave and the external pump, and constitute a characteristic feature which is inherently contained in the steady-state solution given by Eq.(32).

To verify that short wavelength oscillations are indeed excited by the sequence of events shown in Figs. 1 and 2, it is convenient to display the spatial dependence of the real and imaginary parts of A , as is done in Fig. 3 for $\tau=2.5$. It is evident from this figure and Eq.(32) that

$$\text{Re } A \rightarrow - \pi G_i(z) \quad (45)$$

$$\text{Im } A \rightarrow - \pi A_i(z)$$

as time progresses.

To determine the nature of the mode converted oscillations it is convenient to plot a phasor diagram of the type commonly used experimentally to measure the direction of phase propagation. Such a plot is shown in Fig. 4, where one displays the imaginary part of A versus its real part for a fixed time $\tau=2.75$, and with spatial position as the parameter varying along the curve. The direction of the arrows correspond to moving down the density gradient. The fact that the curve in Fig. 4 rotates in the counterclockwise direction (i.e., the direction of increasing phase angle) identifies the mode-converted oscillations as forward waves, i.e., the energy and phase velocities point in the same direction, as is appropriate for Langmuir waves.

Having uncovered the time evolution of the linear mode-conversion process we proceed next to examine its nonlinear modification.

B. Weakly Nonlinear Behavior

It is found that for values of $p < 0.1$ the nonlinear modification of the density profile does not cause any significant changes in the mode-conversion process illustrated in part A of this section. However, in the range $0.1 < p < 0.8$ it is possible to identify an intermediate regime in which the weak nonlinearity causes an adiabatic spatial distortion in the pure Airy pattern given by Eq.(32).

The characteristic distortion observed in this regime, and obtained from Eq.(34), is exhibited in Fig. 5, where we present the spatial dependence of $|A|^2$ for $p=0.5$ (lower curve) and for $p=0$ (upper curve), at the same time $\tau=3.0$. The straight line in Fig. 5 corresponds to the unperturbed density profile, and the slightly curved line below it is the nonlinear counterpart. It is clear from the presentation of Fig. 5 that at this level of nonlinearity the distortion of the profile is quite mild. It consists simply of a small shift of the resonance point into the overdense region (i.e., $z>0$) accompanied by a slight flattening of the density gradient. This modification causes an overall shift in the $|A|^2$ pattern toward $z=0$, as well as a reduction in the peak amplitude.

As is mentioned in Sec. II, in this intermediate regime of pump amplitudes the nonlinear distortion of the mode-conversion pattern can be handled by perturbation theory, i.e., through the iterative solution of Eq.(36). A characteristic result obtained by this procedure is shown in Fig. 6, where we display the spatial dependence of $|A|^2$ for $p=0.5$ (lower curve) and for $p=0$ upper curve. Both curves are obtained for $\Gamma=0$ and correspond to the physical situation encountered as $\tau \rightarrow \infty$. Fig. 6 demonstrates that the adiabatic distortion seen in the time evolution, and shown in Fig. 5, is indeed reproduced by the perturbation theory calculation.

The reasons for the differences seen between Figs. 5 and 6 in the region $z \ll -1$ are: a) the curves shown in Fig. 5 correspond to $\tau=3.0$, hence the mode-

converted waves have not had sufficient time to propagate down the density gradient, and b) the curves in Fig. 5 are obtained from Eq.(34) with $\Gamma=0.2$, hence their peak amplitude is reduced (relative to the $\Gamma=0$ case) and their pattern undergoes an enhanced spatial damping down the density gradient.

We proceed next to discuss the fully nonlinear behavior of the system which can be reached by increasing the pump amplitude beyond the $p=1.0$ level.

C. Nonlinear Behavior Without Ion Inertia

The adiabatic distortion of the Airy-type pattern observed to occur for $p < 0.8$ is radically altered when the pump amplitude is increased beyond the $p=1.0$ level. In this fully nonlinear regime we have not found a suitable convergent technique capable of yielding a self-consistent solution of the steady-state nonlinear integral equation given by Eq.(36). In fact, the time evolution obtained from the numerical solution of Eq.(34), and from the system defined by Eqs.(21) and (22), indicates that such a steady-state may not exist within the present description. The system simply runs continuously through a variety of nonlinear states characterized by relaxation oscillations.

The reason for the strong modification of the linear mode-conversion process at these larger amplitude levels is that localized density cavities or pockets are generated in the plasma by the ponderomotive force. These density cavities cause a partial reflection of the mode-converted waves and also it alters the efficiency of mode-conversion due to the local steepening of the profile.

To illustrate the direct effect produced on the mode-conversion pattern by the appearance of a localized density cavity, we consider the steady-state equation

$$\frac{d^2}{dz^2} A - [z - N(z)]A = 1 \quad (46)$$

with

$$N(z) = \{2.5 \operatorname{sech}[4(z-1)]\}^2 \quad (47)$$

representing a narrow density cavity centered in the initially overdense region. The effect of such a cavity is clearly visible in Fig. 7, where we display the spatial dependence of $|A|^2$. In Fig. 7 curve a) is obtained with $N=0$, hence representing the linear pattern, while curve b) is generated with N given by Eq.(47). The density profile corresponding to Eq.(47) is represented by the slopping line.

It is evident from Fig. 7 that the creation of a cavity in the density profile in the overdense side (i.e., $z>0$) gives rise to a strong localization of the electric field. The spatial localization arises because the cavity provides a potential well within which the Langmuir oscillations can be partially trapped, i.e., they are prevented from convecting down the density gradient. As the degree of trapping increases, so does the peak amplitude of the localized field because its total energy content is determined by the balance between the pumping by the external field and the convection by the Langmuir oscillations. It is seen in Fig. 7 that although the cavity described by Eq.(47) causes the localization of the electric field, it does not give rise to complete trapping, as is made evident by the extended wing of the pattern observed in the region $z<0$.

Although the results shown in Fig. 7 illustrate the basic process involved in the generation of localized electric fields in a nonuniform plasma, it should be realized that an important ingredient is missing in the calculation leading to this figure. Namely, the shape, position, and depth of the density cavity must be self-consistent with the $|A|^2$ it generates. When this restriction is imposed it is found that nonlinear patterns such as that illustrated in Fig. 7 last only for a finite time, but are generated in a repetitive manner, as is shown later on.

In the remaining of this subsection we discuss the self-consistent time evolution of the generation of localized electric fields, as obtained by neglecting the effect of ion inertia in Eq.(22), i.e., we investigate the system by solving Eq.(34) directly.

Fig. 8 displays a typical localized electric field and its self-consistent density cavity obtained for $p=3.0$, $\Gamma=0.2$, at time $\tau=1.75$. It is clear from Fig. 8 that the self-consistent distortion of the profile moves the resonance

layer (i.e., $\text{Re } \epsilon' = 0$) deeper into the plasma, and creates a sharp density cavity centered at the original location of the resonance. Unlike the simulated conditions leading to Fig. 7, the self-consistent density cavity with ion-inertia neglected is unable to create a situation such that $\text{Re } \epsilon'$ has two zero crossings. As a consequence, the localized pattern seen in Fig. 8 does not evolve into a steady-state feature because the Langmuir oscillations are able to leak out of the density cavity and thus convect the energy down the density gradient.

An example of the convection out of the localized density cavity initially centered at $z=0$ is shown in Fig. 9. This figure corresponds to the same parameters used in Fig. 8, but shows the behavior at a later time $\tau=2.8$. It is seen in Fig. 9 that a localized electric field moves down the density gradient and drags a density cavity which prevents it from spreading into an extended pattern. In Fig. 9 it is also observed that another localized field is generated in the region $z>0$. The reason for the reappearance of this feature is that the location where $\text{Re } \epsilon' = 0$ moves into the plasma and the pump field is still turned-on, hence the cold plasma resonance is excited anew, it evolves into a localized field and thus repeats the cycle.

A summary of the three basic stages observed in the nonlinear evolution is shown in Fig. 10, where we display the spatial dependence of $|A|^2$ and of the scaled density profile for various times. The early stage, indicated by $\tau=1.4$ in Fig. 10, consists simply of the secular build-up of the linear cold plasma resonance centered initially at $z=0$. Due to the ponderomotive force, the excitation of the cold plasma resonance generates a density cavity which prevents the linear mode-conversion process from developing, hence giving rise to the second stage represented in Fig. 10 at $\tau=1.7$. During this second stage a localized electric field appears whose width decreases with increasing

amplitude, thus resembling a Langmuir-wave soliton. Since in the absence of ion inertia no density increases or bumps can be generated, this implies that the localized structure generated during the second stage is not confined on the low density side. Accordingly, the localized field begins to propagate down the density gradient. The third stage in the nonlinear evolution is represented by $\tau=2.2$ in Fig. 10. It consists of the propagation of a localized pulse down the density gradient, accompanied by the simultaneous build-up of the cold plasma resonance at a new location deeper into the plasma.

The characteristic events depicted in Fig. 10, although obtained for a zero-order profile which is chosen as a linear function of position, are independent of this particular choice. To verify the generality of the nonlinear behavior seen in Fig. 10 we have investigated a variety of zero-order profiles. An interesting unperturbed density we have considered is

$$\frac{n_o(z)}{n_p} = z + \exp[-(z+5)^2/5] - \exp[-(z-5)^2/5] \quad (48)$$

which is non-monotonic and contains a zero-order cavity as well as a bump. A characteristic result obtained for $p=6.0$, $\Gamma=0.2$ is shown in Fig. 11. The continuous slopping curve corresponds to the unperturbed profile while the dashed curve corresponds to the nonlinearly modified profile. It is seen in Fig. 11 that significant structures develop in two spatially separated regions in the neighborhood of $\text{Re } \epsilon'=0$. The localized field on the low density side consists only of a single peak because there is a finite wave leakage down the density gradient. The structure located deeper into the plasma consists of several neighboring localized peaks because the existence of a zero-order density cavity stops the wave-leakage. As a consequence of the development of localized electric fields on both sides of the initial density bump, the unperturbed profile evolves in time into a plasma with two sharp gradients connected by a flat portion within which a strong level of spiky turbulence exists.

We proceed next to investigate the generation of density cavities and localized electric fields with ion inertia included.

D. Nonlinear Behavior with Ion Inertia

The effect of ion inertia on the process of generating density cavities and localized electric fields appears in Eqs.(21) and (22) through the parameter $V = (M/m)^{1/2} (k_D L)^{-1/3}$. In practice this quantity can be quite large depending on the specific parameters of the experiment, e.g., $V \approx 4$ for a hydrogen plasma with $k_D L \approx 10^3$. However, from the numerical standpoint it is not convenient or interesting to consider large values of V because a significant amount of computer time is wasted in following phenomena which are nearly constant in time. For this reason the results to be presented have been obtained with a value of $V=2.0$ and using a delay between the ion and electron time meshes of $d=4$, as indicated in the numerical scheme of Eq.(41). The usage of such a low value of V can be interpreted as an exact treatment of a physical situation dealing with an extremely gentle density gradient, or alternatively, as viewing a realistic problem with a camera which has been artificially speeded-up.

Fig. 12 displays the characteristic time evolution of the system described by Eqs.(21) and (22) over the intervals $-20 \leq z \leq 5$ and $3.0 \leq \tau \leq 5.0$ for $p=3.0$, and $\Gamma=0.2$. This figure is to be compared with its counterpart, Fig. 10, which is generated from Eq.(34) for the same p and Γ .

The first difference which becomes apparent in Fig. 12 is the slower evolution of the nonlinearity when ion inertia is included, as is expected. The early appearance of the nonlinearity observed in Fig. 10 at $\tau=1.7$ becomes visible in Fig. 12 at $\tau=3.0$. Due to the later appearance of the nonlinearity, the $\tau=3.0$ pattern in Fig. 12 shows clear evidence of the prior development of linear mode-conversion occurring in the essentially linear stage for $\tau < 3.0$.

Another expected difference which shows up clearly in Fig. 12 is that the ponderomotive force now generates density bumps as well as density cavities. This additional feature implies that as the initial density cavity centered at $z=0$ develops, it kicks the excess density up and down the density gradient.

As a consequence of this density rearrangement it is now possible to generate spatial regions which are bounded by two zeroes of $\text{Re } \epsilon'$, as is seen at $\tau=4.0$. The momentary generation of such regions causes the electric field to be more localized, as is seen in the transition from $\tau=4.5$ to 5.0.

An interesting effect which is amenable to direct experimental verification consists of the fission of large individual density cavities into smaller sub-cavities, as is seen at $\tau=4.5$ and 5.0. This splitting is associated with the fact that the temporary barrier created by the density bump can not hold the RF energy on the low density side of the gradient for a long time. Hence, after a certain time the RF energy begins to leak out on this side leaving behind a smaller cavity.

An additional new feature appearing in Fig. 12 is the clear increase in the steepness of the profile in the neighborhood of $z=0$. This behavior is associated with the fact that when ion inertia is included in the process, the shape of the nonlinear density cavity is no longer the mirror image of $|A|^2$, as is seen at $\tau=5.0$ in Fig. 12.

An interesting type of measurement which is quite often used in the laboratory consists of sampling the properties of a process in time at a fixed spatial location, as can be done with a stationary probe or with a sampling electron beam. This type of information is also available in the solution of Eqs.(21) and (22) and provides a slightly different view of the nonlinear evolution which is amenable to experimental verification.

Fig. 13 displays the time evolution of the fluctuation in density at $z=-2.1$, which corresponds to a point located on the underdense side of the resonant layer. The parameters used correspond to those of Fig. 12. It is seen in Fig. 13 that the local density remains unperturbed up to $\tau=1.71$, and thereafter it begins to decrease steadily up to a minimum level. This process

corresponds to the formation of the density cavity initially centered at $z=0$. After $\tau=3.98$ the magnitude of the density cavity decreases and significant density fluctuations of the ion-acoustic type are excited.

The corresponding behavior on the overdense side of the resonant layer is shown in Fig. 14 for $z=3.0$. It is seen in this figure that the local density remains essentially unperturbed up to a time $\tau=1.14$ beyond which it proceeds to increase steadily. This increase in density is associated with the digging of a density hole around $z=0$. Later in time, at $\tau=3.42$, it is observed that the monotonic increase in density exhibits a modulation of the ion-acoustic type whose amplitude increases in time.

The combined picture which emerges from Figs. 13 and 14 is that the ponderomotive force digs a hole in the underdense side of the resonant layer, and in doing so it throws the excess initial density away from the $z=0$ point. Since in this process the plasma is shaken, it responds to this perturbation by generating ion-acoustic fluctuations that propagate up and down the density gradient.

Another quantity which is of experimental interest is the local time evolution of the electric field. A display of such behavior is shown in Fig. 15 for a point $z=-1.1$, located on the underdense side for the conditions corresponding to Figs. 12, 13, and 14. Fig. 15 indicates that in the interval $\tau < 1.71$ $|A|^2$ builds-up in a secular manner, as expected due to the excitation of the cold plasma resonance. Around $\tau = 1.71$ the secular growth stops due to the appearance of the mode-conversion process which shifts the pattern down the density gradient. After saturation due to wave convection the local amplitude proceeds to decrease in the interval $2.28 < \tau < 3.42$ due to the localization of the electric field at a point located deeper into the plasma. As has been seen on several occasions in this study, the cold plasma resonance continues

to be excited, thus the cycle repeats. As is seen in Fig. 15, this cycle manifests itself locally in the form of deep relaxation oscillations which are amenable to experimental verification.

The counterpart of the relaxation oscillations exhibited in Fig. 15 is shown in Fig. 16 for a fixed location on the overdense side $z=1.3$. On this side of the resonance no relaxation oscillations are observed because no density cavities are regenerated in this region. Fig. 16 indicates that at this point the cold plasma resonance builds-up in a secular manner up to $\tau=1.14$, and it saturates due to the wave convection down the density gradient. However, the local electric field amplitude does not settle down to a steady level after this event. Instead, it decreases monotonically. This enhanced decrease is a nonlinear effect that arises due to the fact that the density increases monotonically in time in this region, as is demonstrated in Fig. 14. Accordingly, this local position becomes increasingly overdense and leads to the steady decrease in the local field amplitude because of the corresponding decrease in the evanescence length.

V. CONCLUSIONS

This investigation has shown that a simple model based on the nonlinear Schrodinger equation and the ion-acoustic wave equation is capable of describing the detailed space-time evolution of the generation of density cavities and localized electric fields due to the interaction of long wavelength radiation with a nonuniform plasma.

The formation of such nonlinear structures can play an important role in the absorption of electromagnetic radiation in a nonuniform plasma because the localized fields can act as powerful electron accelerators that generate suprathermal tails¹⁰ in the electron velocity distribution function. Also, in the process of forming the density cavities bursts of fast ions can be created. Absorption mechanisms of this type have been observed in computer simulations⁸ as well as in laboratory experiments¹¹.

The present formulation predicts that one must contend with this type of nonlinear phenomena for external power levels such that the nonlinear parameter $p = (\omega L / \bar{v}_e)^2 (E_0^2 / 12\pi n_p T) > 1$. Below this power level, the present study shows that the physics of the problem is dominated by the process of linear mode-conversion. Accordingly, in the low power level regime the dominant absorption mechanism consists of linear Landau damping of the mode-converted waves as they propagate down the density gradient.

The present time dependent formulation has permitted the description of the time evolution of the linear mode-conversion process. This process has been previously^{1,2} investigated in considerable detail, but only in its steady-state form. Therefore, the present results expand and compliment the previous investigations by showing how linear mode-conversion takes place, and that asymptotically in time the spatial pattern associated with this process approaches the Airy-type waveforms. The present study goes beyond the strictly

linear regime by showing that for mild nonlinearity the Airy-type of pattern is adiabatically distorted, and further that such distortion attains a steady-state which is fully describable by perturbation theory for external power levels such that $p < 0.8$.

The inclusion of ion inertia effects in the present study complements a previous investigation⁴ in which such an effect was neglected for the sake of simplicity. The present results show that the inclusion of ion inertia does not alter the important features found in the earlier study. Density cavities and localized electric fields are indeed generated, but the details of the process are slightly different. Additional new phenomena, such as the excitation of oscillations of the ion-acoustic type after the formation of a density cavity, are uncovered.

The present model predicts the existence of interesting relaxation oscillations in the underdense side of the resonance layer, and an initial build-up of the electric field on the overdense side, which is followed by a long term enhanced decay. These features can be traced to the redistribution of density up and down the gradient and are amenable to experimental study. Under well controlled laboratory conditions these features can be detected with a small probe or with a sampling electron beam. In a laser-plasma experiment these effects may manifest in the form of modulation of the light absorption, or equivalently, in the appearance of sidebands in the light reflected from the resonant layer.

In summary, the present model has proven its usefulness by the ability to encompass a wide variety of physical phenomena of great interest under a simple mathematical structure. Whether or not this type of approach can be extended to describe more complicated phenomena hinges on the ability to incorporate the effect of single particle acceleration into the nonlinear Schrodinger equation, a topic which deserves more attention.

ACKNOWLEDGMENT

This work has been supported by the Office of Naval Research through
Grant ONR N00014-75-C-0476 P00002 and the National Science Foundation
NSF PHY 75-07809.

BIBLIOGRAPHY

1. A. D. Piliya, Zh. Tekh. Fiz. 36, 819 (1966) [Sov. Phys. Tech. Phys. 11, 609 (1966)].
2. D. L. Kelly and A. Banos, Jr., UCLA Plasma Physics Group Report PPG-170 (1974).
3. H. C. Kim, R. Stenzel, and A. Y. Wong, Phys. Rev. Lett. 33, 886 (1974).
4. G. J. Morales and Y. C. Lee, Phys. Rev. Lett. 33, 1016 (1974).
5. G. J. Morales and Y. C. Lee, APS Bull. 19, 861 (1974).
6. A. Y. Wong and W. DiVergilio Private Communication to be Published.
7. Handbook of Mathematical Functions, Edited by M. Abramowitz and I. A. Stegun (Dover, New York, 1970), p. 444.
8. K. Estabrook, E. Valeo, and W. Kruer, Phys. Letters 49A, 109 (1974).
9. D. Potter, Computational Physics (Wiley, New York 1973) p. 88.
10. G. J. Morales and Y. C. Lee, Phys. Rev. Lett. 33, 1534 (1974).
11. A. Y. Wong and R. L. Stenzel, Phys. Rev. Lett. 34, 727 (1975).

FIGURE CAPTIONS

- FIG. 1 Early excitation of the cold plasma resonance observed over the interval $0.5 \leq \tau \leq 1.5$. Slopping line represents $\text{Re}(-\epsilon')$, or equivalently, the scaled density profile.
- FIG. 2 Development of thermal convection in the mode-conversion process over the interval $2.0 \leq \tau \leq 3.0$. Slopping line represents $\text{Re}(-\epsilon')$, or equivalently, the scaled density profile.
- FIG. 3 Spatial dependence of the real and imaginary parts of A at $\tau=2.5$. Slopping line represents $\text{Re}(-\epsilon')$, or equivalently, the scaled density profile.
- FIG. 4 Phasor plot of A at $\tau=2.75$. Counterclockwise winding shows mode-converted wave is of the forward type.
- FIG. 5 Typical adiabatic distortion obtained from Eq.(34) in the weakly nonlinear regime at $\tau=3.0$, $\Gamma=0.2$, and for $p=0$ (linear) and $p=0.5$ (nonlinear). Slopping lines represent $\text{Re}(-\epsilon')$, or equivalently, the scaled density profiles.
- FIG. 6 Steady-state adiabatic distortion obtained from perturbation theory based on Eq.(36) for $\Gamma=0$, and $p=0$ (linear), $p=0.5$ (nonlinear). Slopping lines represent $\text{Re}(-\epsilon')$, or equivalently, the scaled density profiles. To be compared with Fig. 5.
- FIG. 7 Steady-state linear mode-conversion pattern for: a) linear density profile, b) linear density profile with a density cavity, as shown by the slopping line. Profile is not self-consistent with electric field.
- FIG. 8 Typical self-consistent electric field and associated density cavity obtained from Eq.(34) at $\tau=1.75$ for $p=3.0$, $\Gamma=0.2$. To be compared with Fig. 7.

- FIG. 9 Convection of a localized electric field down the density gradient and regeneration of a new resonance obtained from Eq.(34) at $\tau=2.8$, $p=3.0$, $\Gamma=0.2$.
- FIG. 10 Three different stages of evolution observed in the nonlinear regime: a) cold plasma resonance $\tau=1.4$, b) spatial localization $\tau=1.7$, and c) convection and regeneration $\tau=2.2$.
- FIG. 11 Multiple generation of localized electric fields in a nonmonotonic zero order profile for $p=6.0$, $\Gamma=0.2$. Continuous slopping curve refers to the zero order profile. Dashed curve is the self-consistent nonlinear profile.
- FIG. 12 Generation of localized electric fields and density cavities with ion inertia included over the interval $3.0 < \tau < 5.0$ for $p=3.0$, $\Gamma=0.2$, $V=2.0$.
- FIG. 13 Time evolution of the density fluctuations observed at the fixed spatial location $z=-2.1$, on the initially underdense side.
- FIG. 14 Time evolution of the density fluctuations observed at the fixed spatial location $z=3.0$, on the initially overdense side.
- FIG. 15 Time evolution of the electric field amplitude at the fixed spatial location $z=-1.1$, on the initially underdense side.
- FIG. 16 Time evolution of the electric field amplitude at the fixed spatial location $z=1.3$, on the initially overdense side.

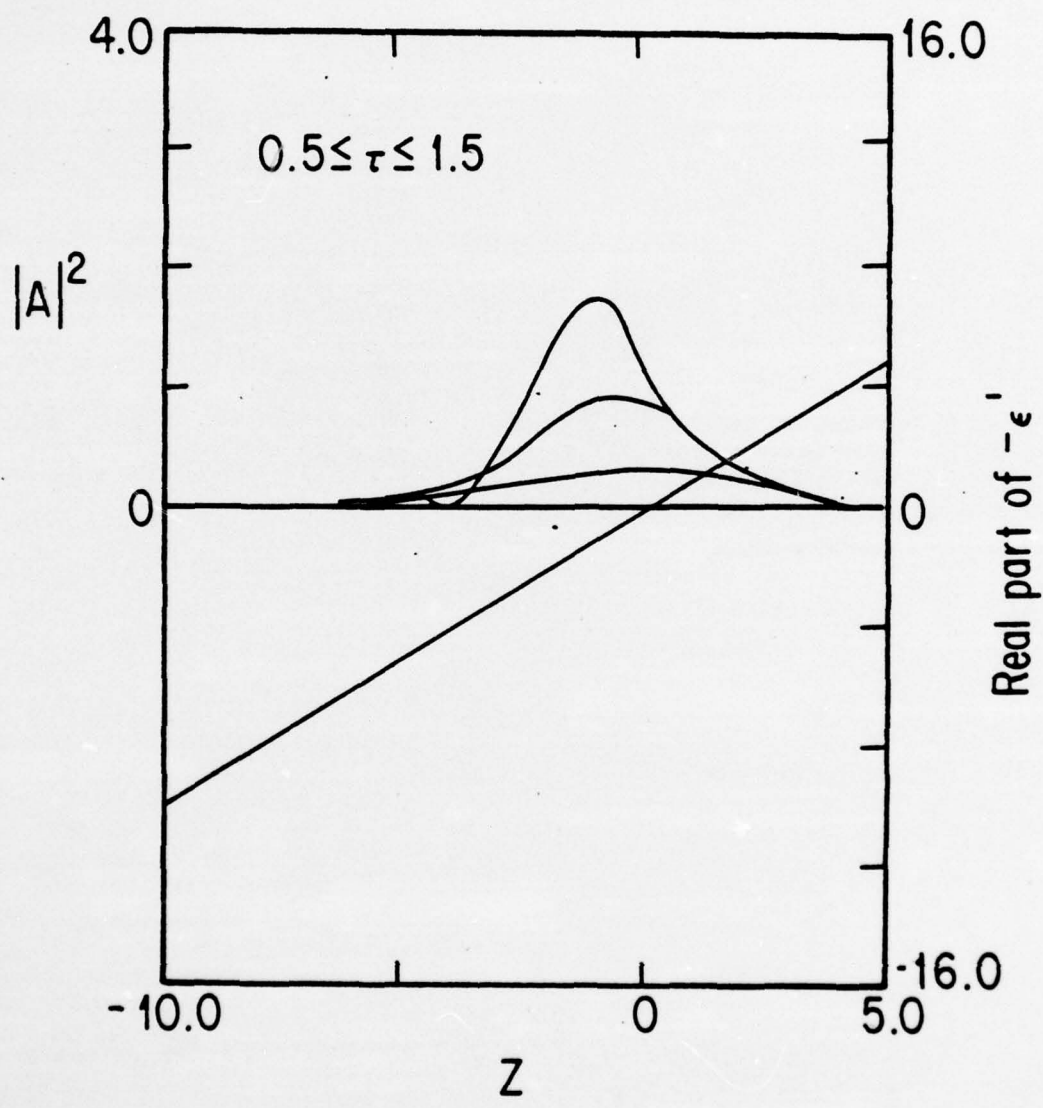


FIGURE 1

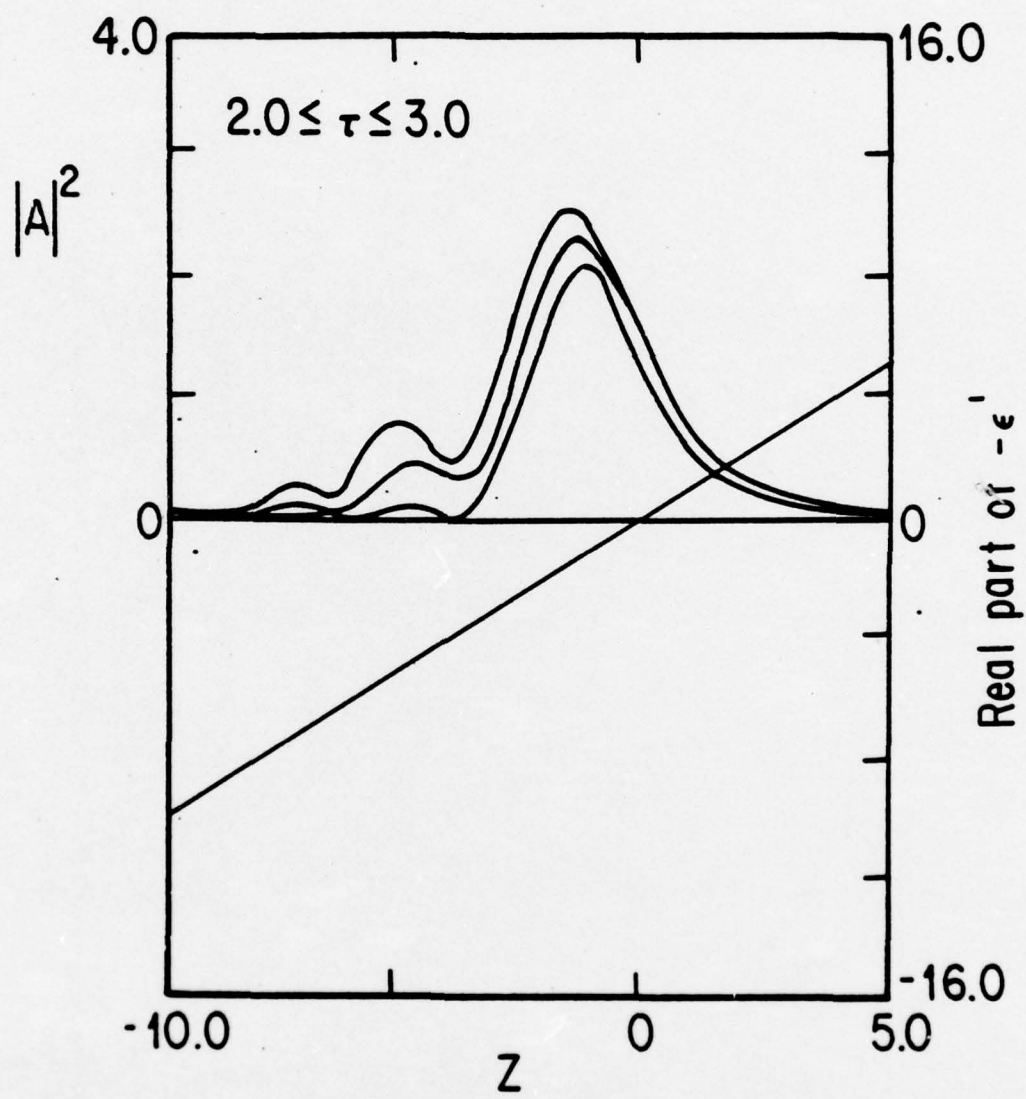


FIGURE 2

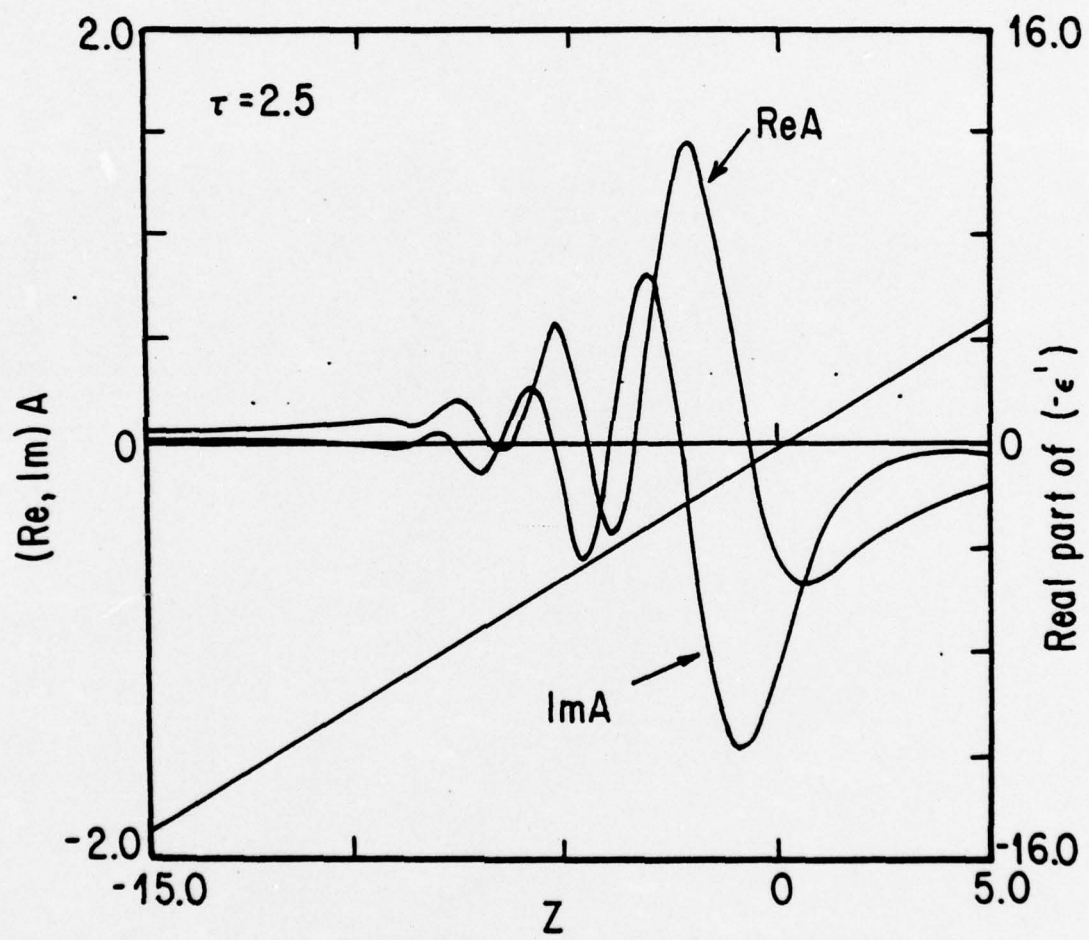


FIGURE 3

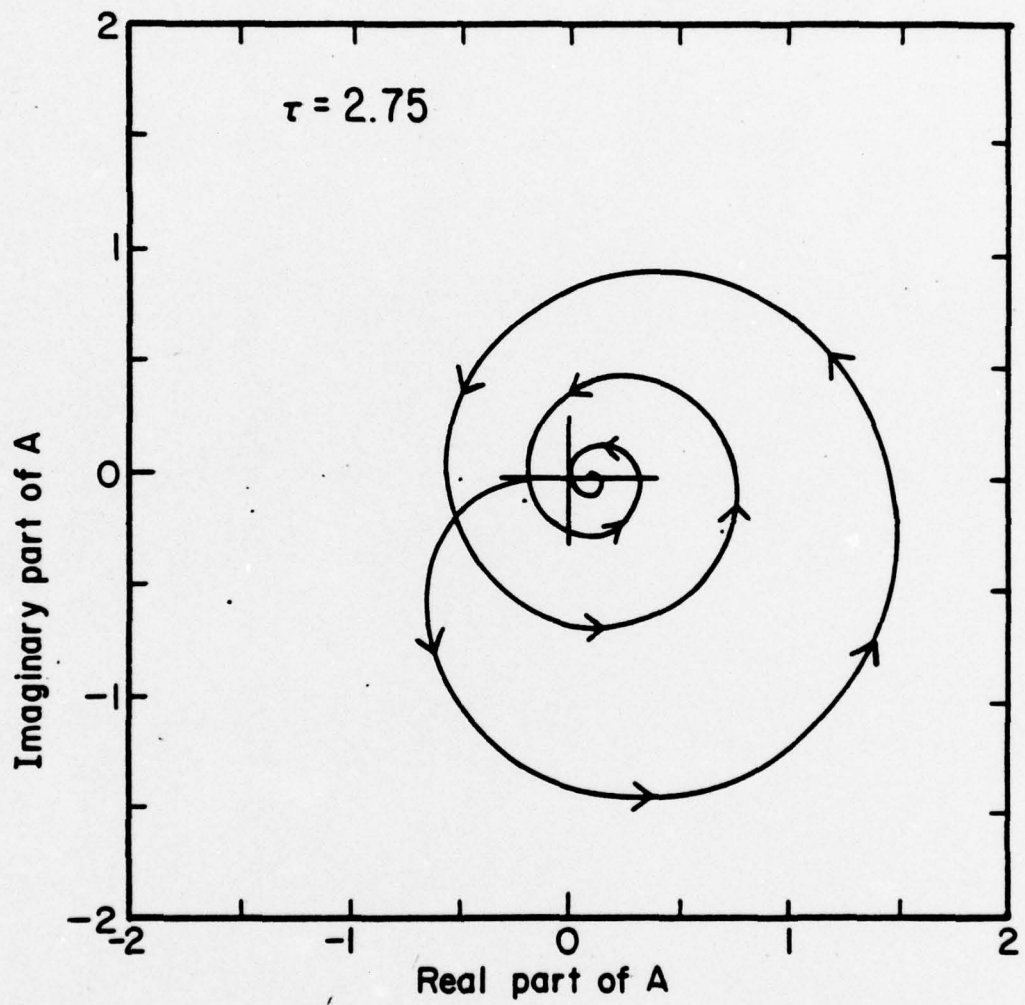


FIGURE 4

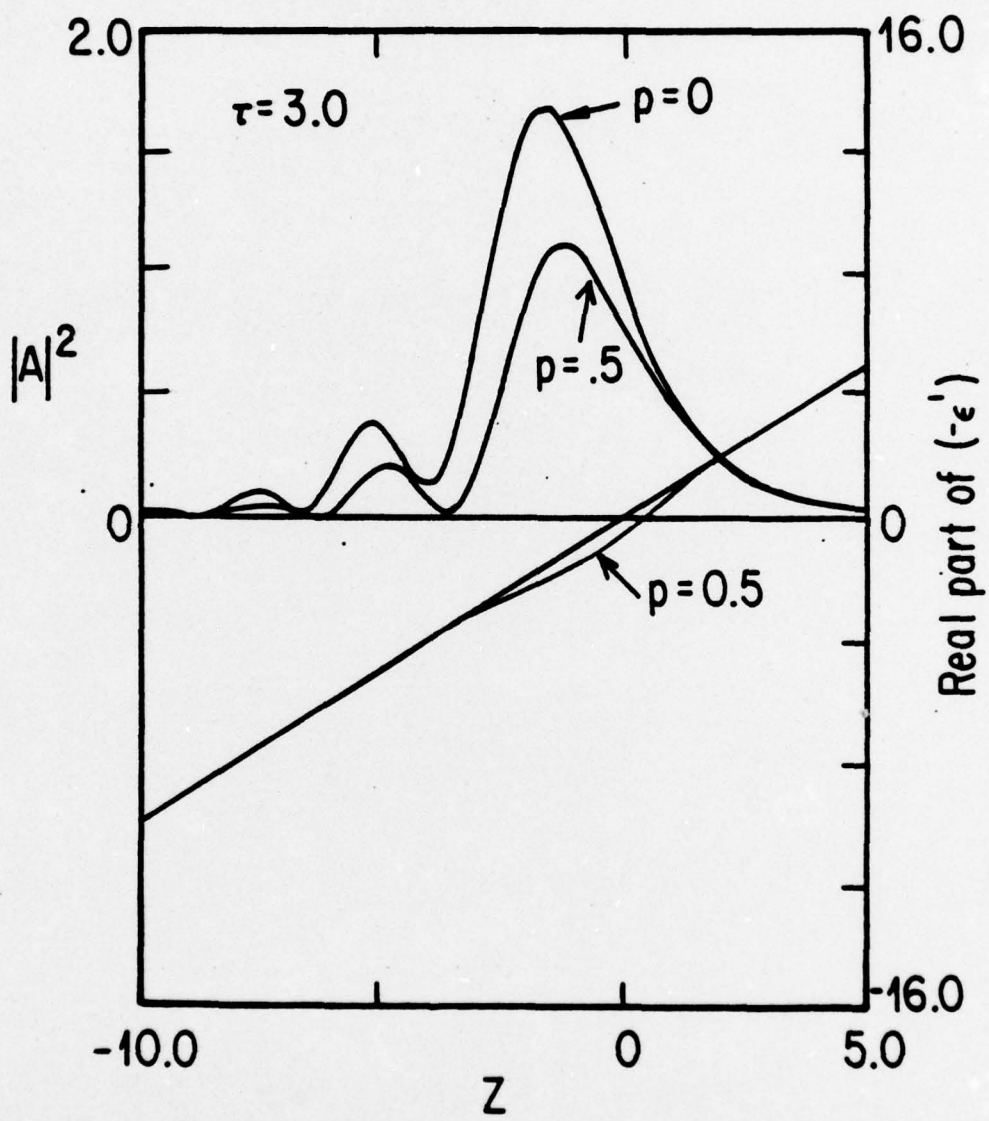


FIGURE 5

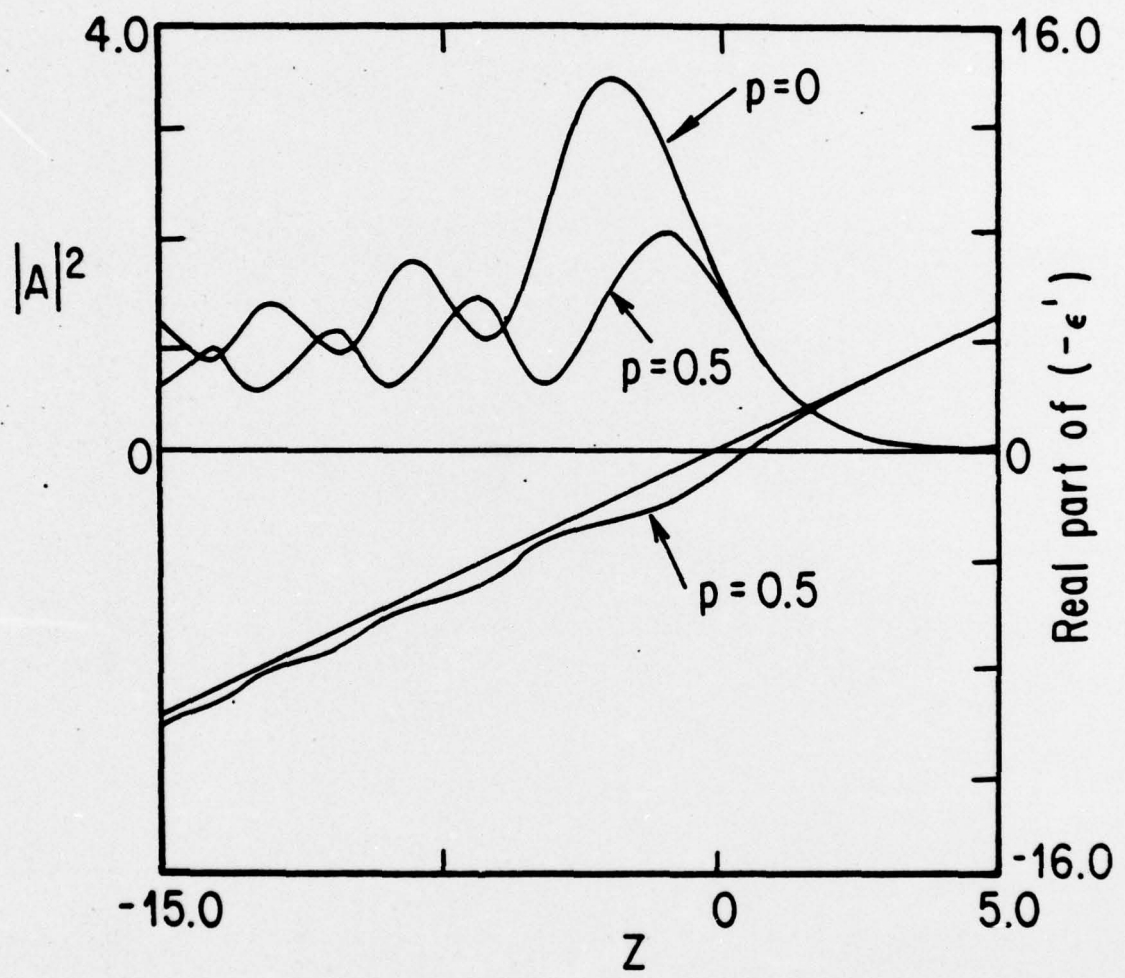


FIGURE 6

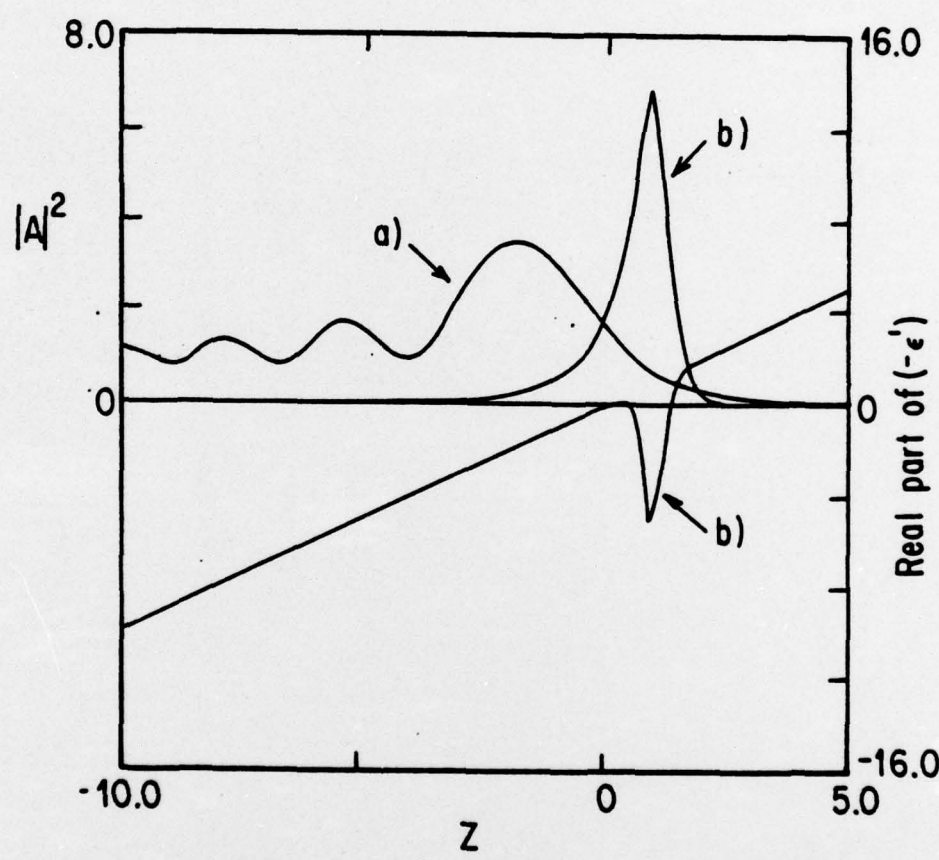


FIGURE 7

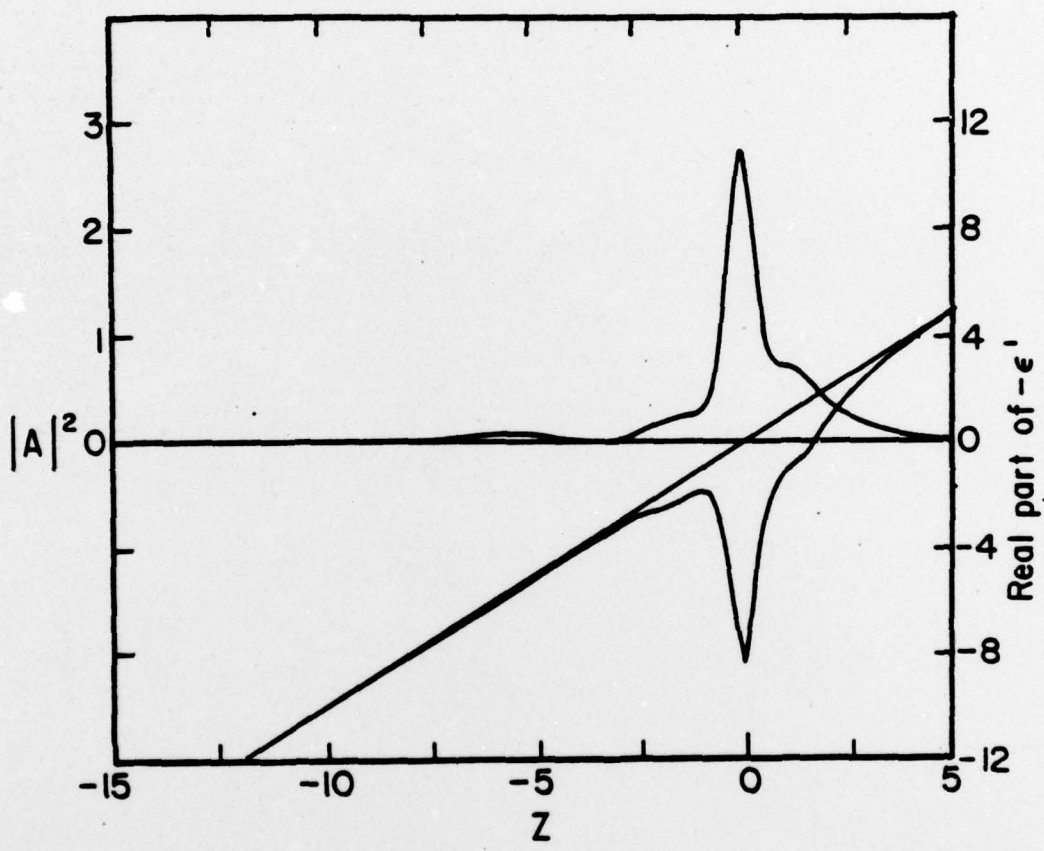


FIGURE 8

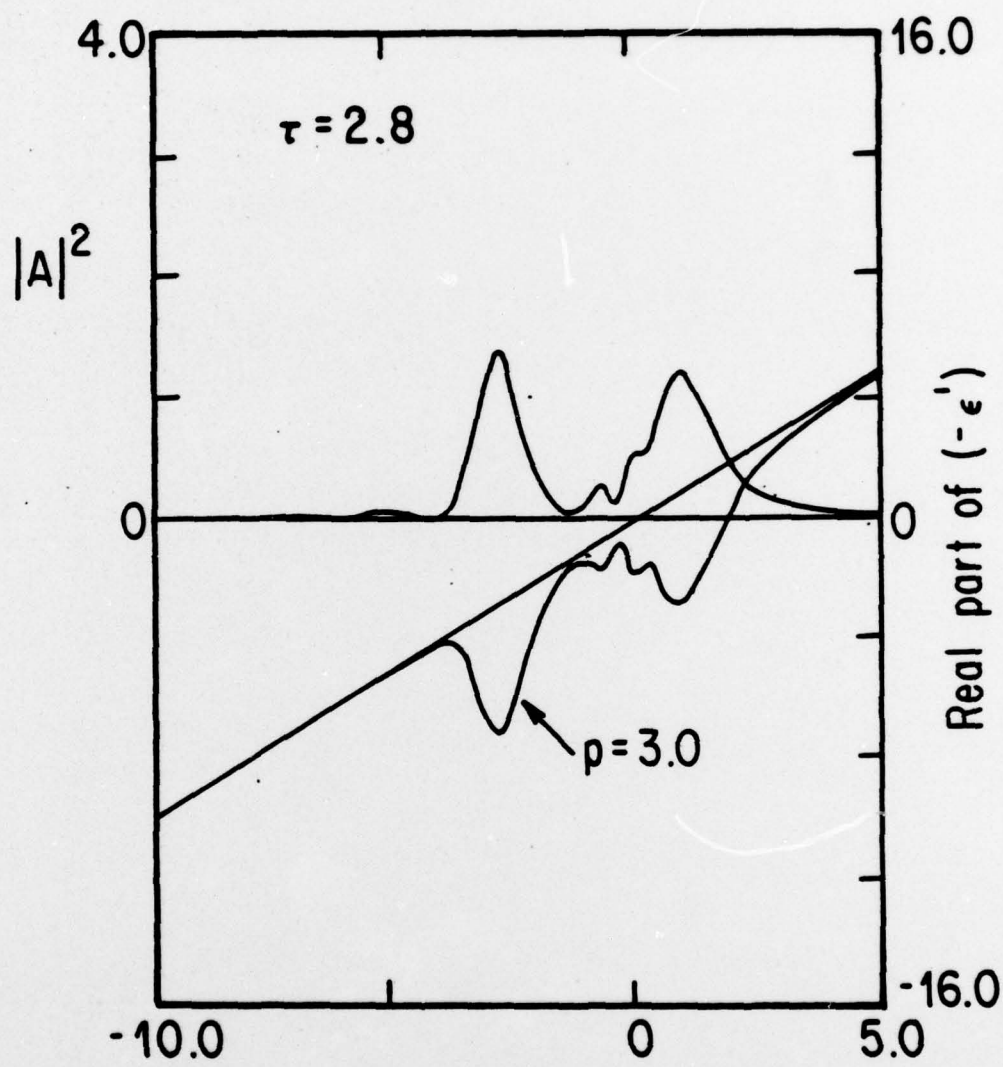


FIGURE 9

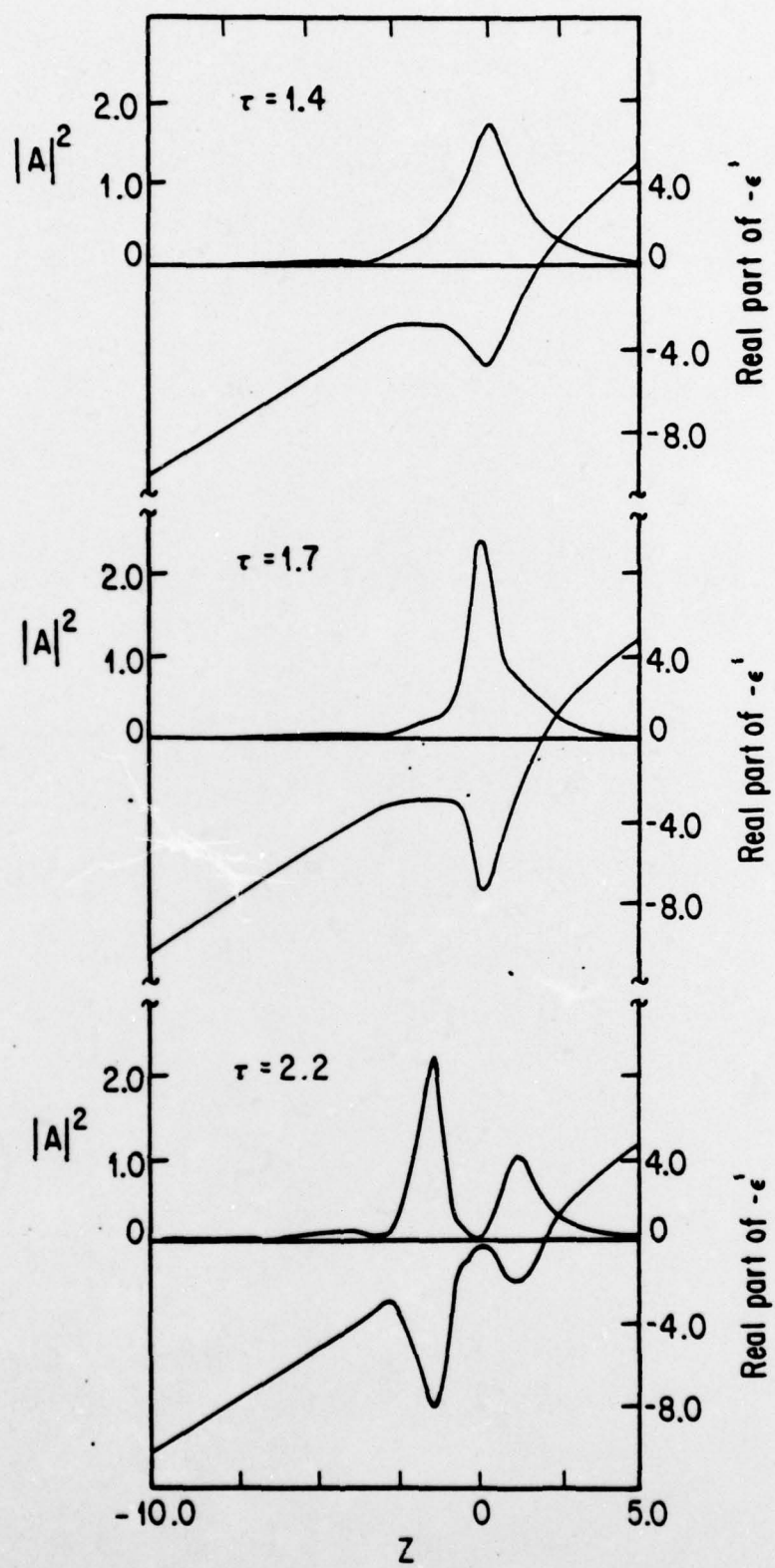


FIGURE 10

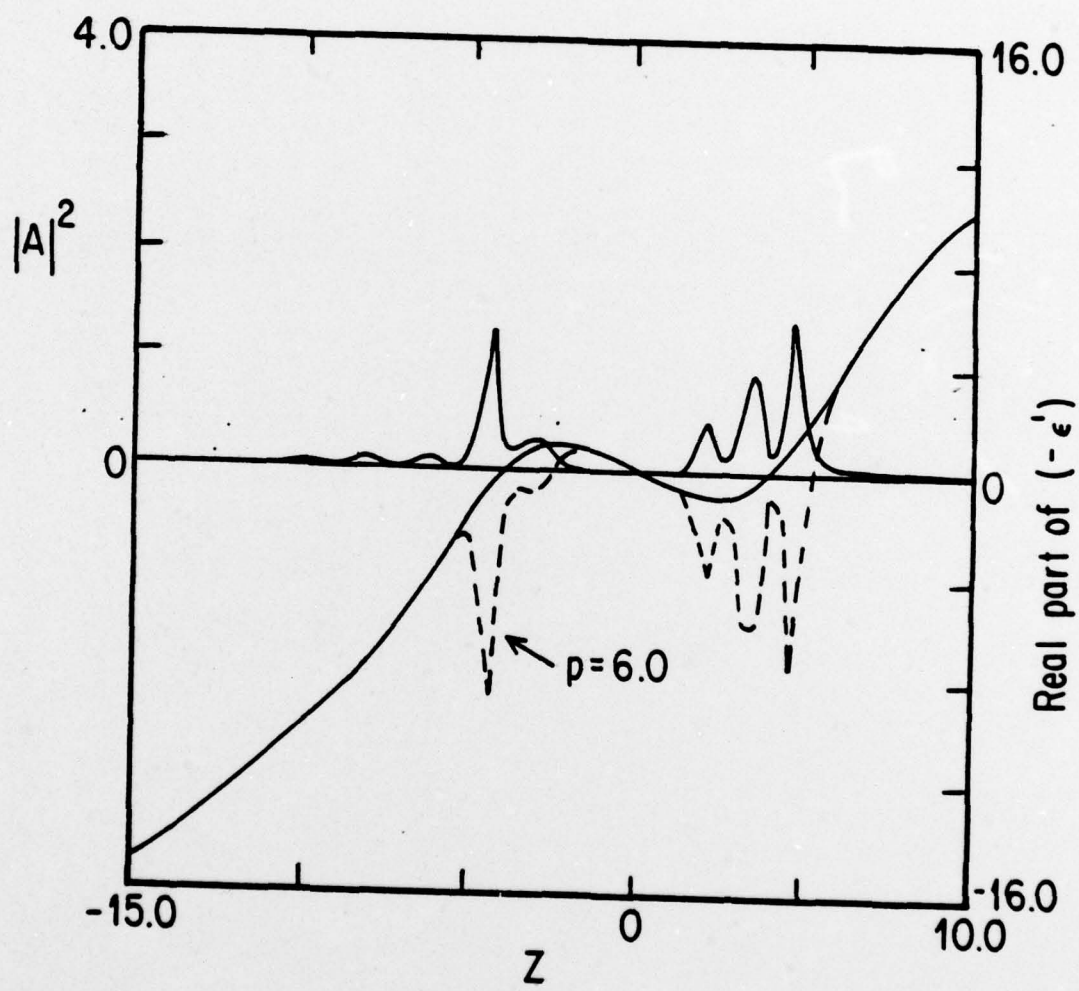


FIGURE 11

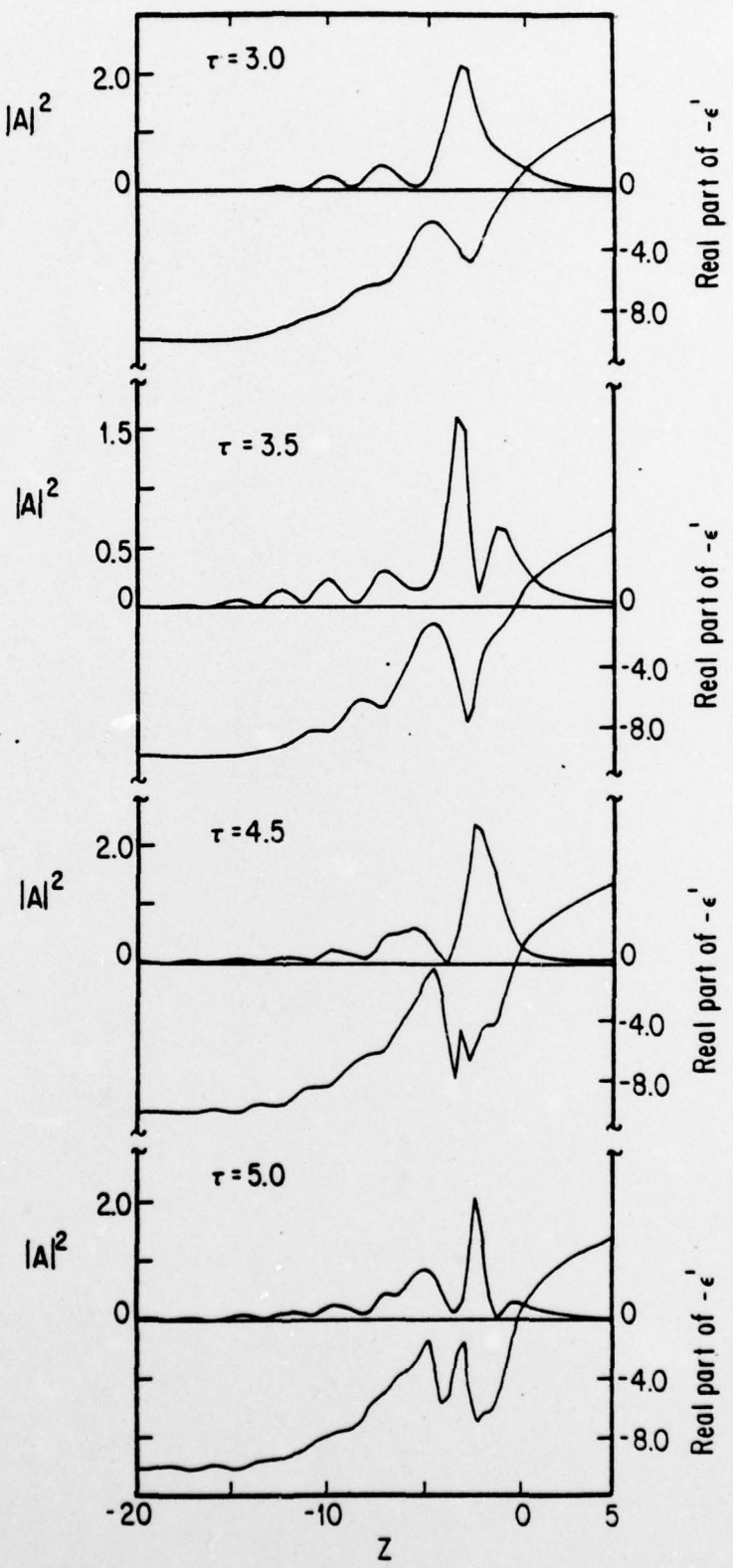


FIGURE 12

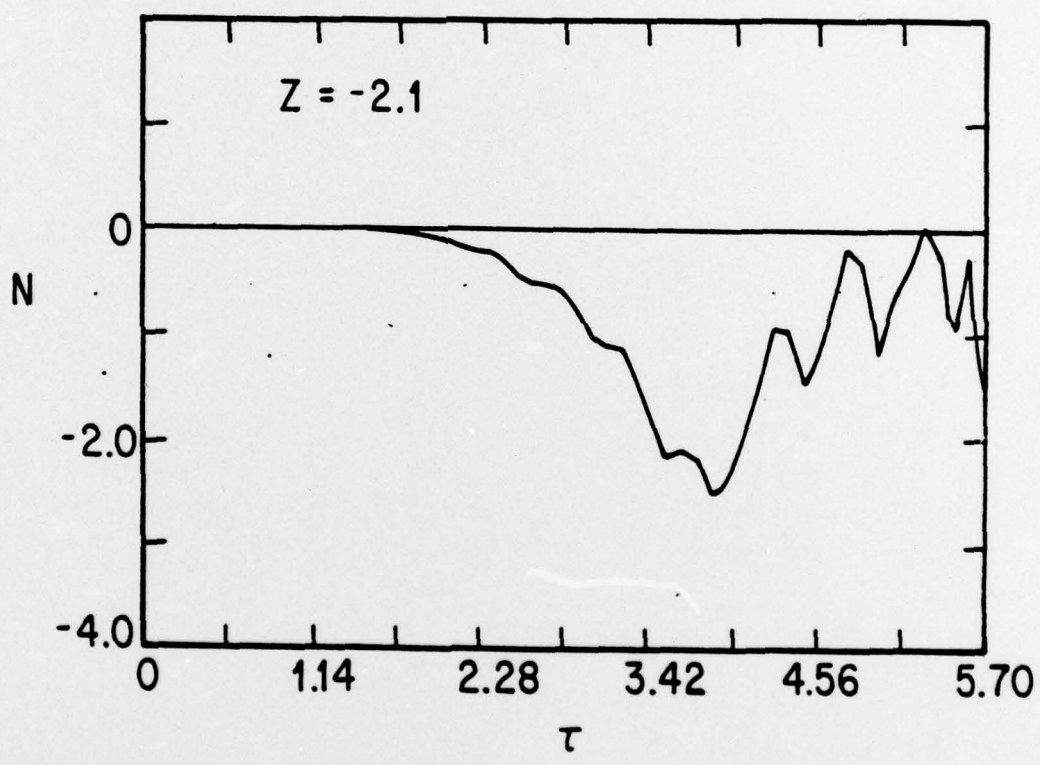


FIGURE 13

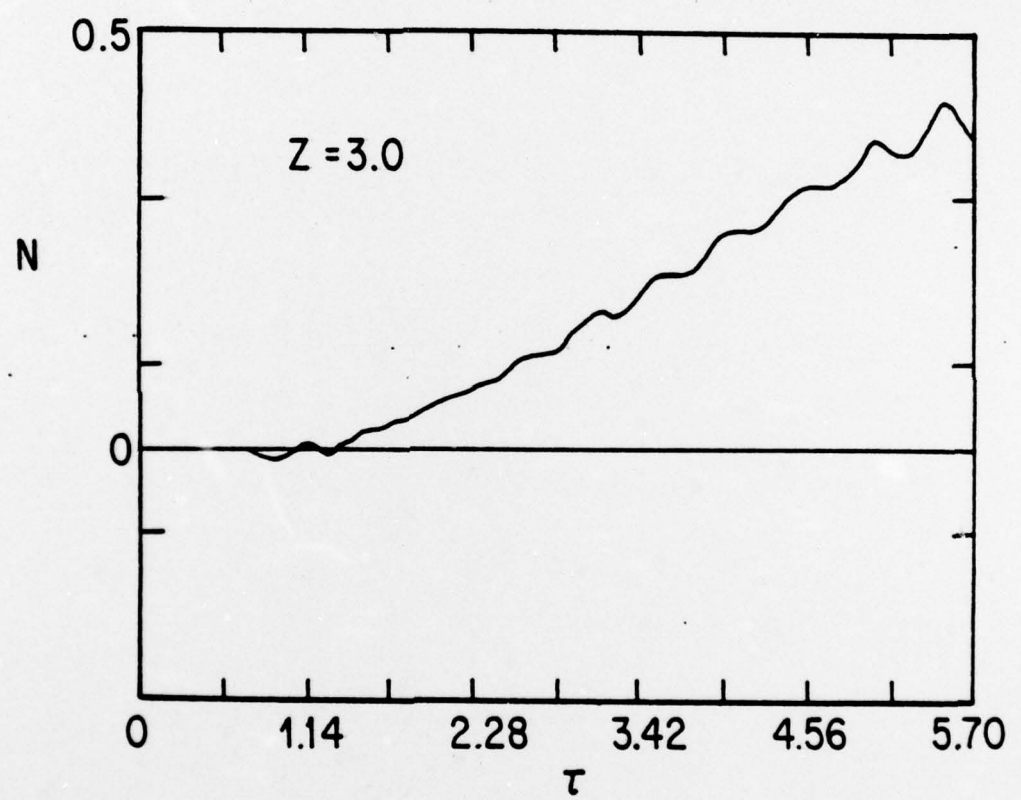


FIGURE 14

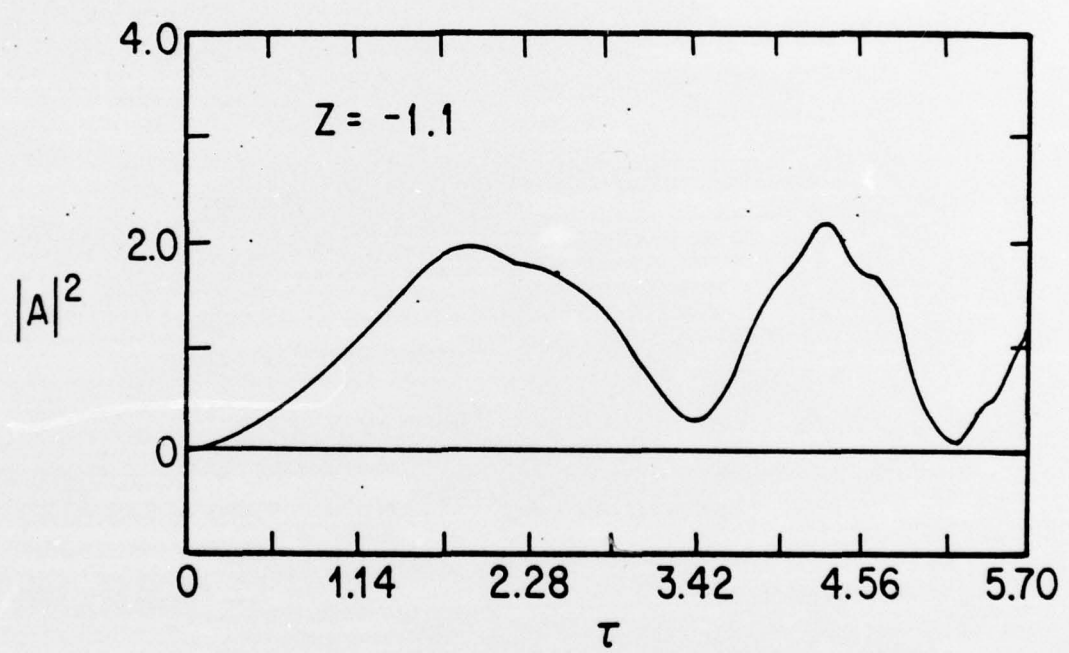


FIGURE 15

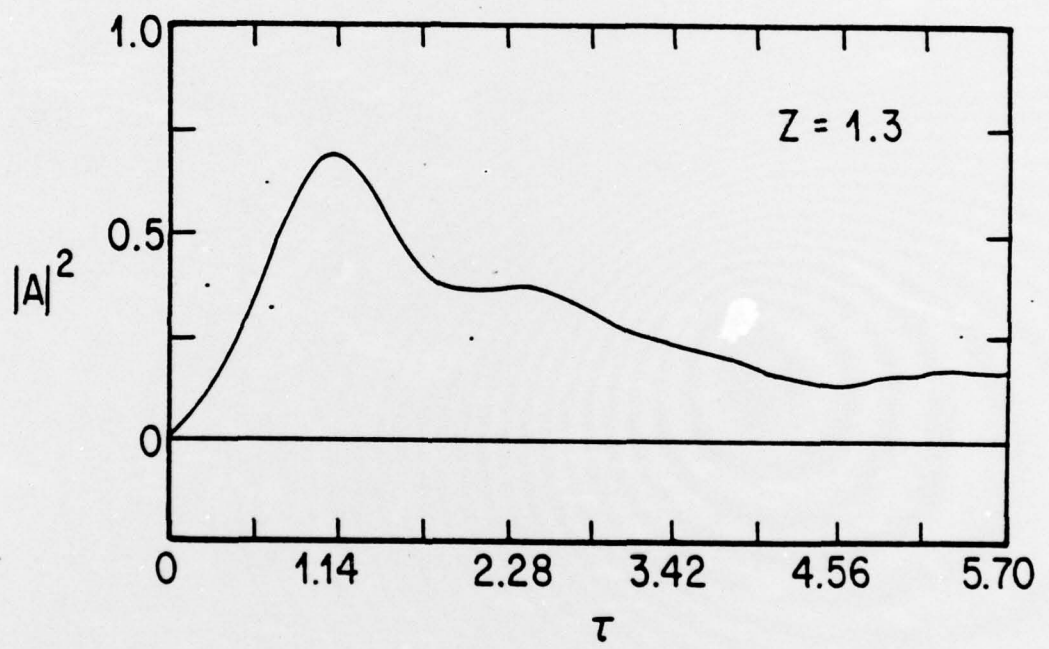


FIGURE 16

LA PLASMA PHYSICS GROUP REPORTS

- UCLA PLASMA PHYSICS GROUP REPORTS**

PPG-69 "Turbulence Structure of Finite Beta Perpendicular Fast Shocks", J. Geophys. Res., **75**, 7007 (1970)(F.V. Coroniti).

PPG-70 "Decay of Ion Acoustic Waves and Formation of Collisionless Electromagnetic Shocks", Phys. Rev. Lett., **25**, 1762 (1970)(C.S. Liu and A.Y. Wong).

PPG-71 "A Method of Studying Trapped Particles and Behavior in Magnetic Geometries", Phys. Rev. Lett., **25**, 1762 (1970)(C.S. Liu and A.Y. Wong).

PPG-72 "The Kinetic Equation for an Unstable Plasma in Parallel Electric and Magnetic Fields", Proc. of Computer Graphols, 136 (1970)(B.D. Fried).

PPG-73 "Kinetic Equation for an Unstable Plasma in Parallel Electric and Magnetic Fields", Phys. Fluids **9**, 1084 (1966)(B.D. Fried and C.A. Yih).

PPG-74 "Stability Limits for Longitudinal Waves in Ion Beam-Plasma Interaction", Phys. Fluids **9**, 2626 (1966).

PPG-75 "Long-Frequency Spatial Response of a Collisionless Electron Plasma", Phys. Fluids **9**, 1261 (1966)(A.Y. Wong).

PPG-76 "Interaction Between Ion Beams and Plasmas", Phys. Rev. Soc. Am., **11**(2) (1958)(A.Y. Wong, D. Judd and M. Sillman).

PPG-77 "Interaction of Cyclotron Echoes from a Highly Ionized Plasma", Phys. Rev. Lett., **21**, 1357 (1968)(D.E. Kaplan and R.M. Hill).

PPG-78 "Excitation and Damping of Drift Waves", Phys. Rev. Lett., **18**, 520 (1967)(A.Y. Wong and R. Rosner).

PPG-79 "The Guiding Center Approximation in Lowest Order", J. Plasma Phys., **3**, 355 (1967)(A. Banos, Jr.).

PPG-80 "Plasma Streaming into a Magnetic Field", Dissertation, Jilin University (1966).

PPG-81 "Cooperative Effects in Plasma Echo Phenomena", Proc. of Int'l. Conf. on Quasistationary Plasmas, Frascati, Rome, 1967.

PPG-82 "Quasi-Mechanical Theory of Grid Excitation of Low Frequency Waves in a Plasma", Dissertation, April (1967)(G.I. Lincoln and Nonlinear.

PPG-83 "The Expansion and Diffusion of an Isolated Plasma Column", Dissertation, May (1967)(J.S. Hyman).

PPG-84 "Two-Pole Approximation for the Plasma Dispersion Function", Phys. Fluids **11**, 249 (1968)(B.D. Fried, C.L. Hirsch and J. McCullough).

PPG-85 "Experimental Investigation of Electron Runaway Phenomena", Dissertation, August (1967)(J.S. DeGroot).

PPG-86 "Parametric Coupling of Two-Dimensional Drift Waves", Proc. of 2nd Inst'l. Conf. on Fluctuations and Diffusion in Plasmas, Jane October (1967)(F. Haft, R. Rosher and A.Y. Wong).

PPG-87 "Cyclotron Echoes from Drift Effects", Phys. Rev. Lett., **20**, 318 (1968)(D.O.R. Baker, N. Ahern and A.Y. Wong).

PPG-88 "Wave Echoes", Phys. Rev. Letters, **21**, 1360 (1968)(A.Y. Wong).

PPG-89 "Cyclotron Echoes in Plasmas", Dissertation, March (1967)(M.E. Rensink).

PPG-90 "Particulate Turbulence in Shock Waves of the Magnetosphere", R. Carvalho, J.F. McClellan and H.R. Rudolphi, eds., October (1967)(H. R. Rangwani).

PPG-91 "The Inhomogeneous Two-Stream Instability", September (1967)(G. Knorr).

PPG-92 "Magnetic Resonance Penetration in High Beta Plasmas", J. Plasma Phys., **3**, 55 (1969) (V. Ferri and C. S. Ossakow).

PPG-93 "Magnetic Resonance Penetration Across a Magnetic Field", Phys. Fluids **12**, 702 (1969)(B.D. Fried and C.F. Kennel).

PPG-94 "Resonant Status Transitions", Feb. 1, 1967-Jan. 31, 1968 (Principal Investigators, A. Banos, Jr., B.D. Fried, and C.F. Kennel).

PPG-95 "The Theoretic's Magnetosphere", Edinburgh, 1969 Vol. I (C.F. Kennel).

PPG-96 "Electromagnetic Pitch Angle Instabilities in Space", Plasma Waves in Space and in the Laboratory, ed. J.O. Thomas and K.J. Lambark (Eduardo U. Press, Edinburgh, 1969) Vol. II (C.F. Kennel and F.L. Scarf).

PPG-97 "Electromagnetic Echoes in Collisionless Plasmas", Phys. Fluids **12**, 860 (1969)(A.Y. Wong).

PPG-98 "Parametric Excitation of Ulrit waves in a Resistive Plasma", Phys. Fluids **12**, 1967 (1969)(A.Y. Wong).

PPG-99 "Parametric Excitation of Thermal Fluctuations at Plasma Drift Wave Frequencies", Phys. Rev. Lett., **21**, 516 (1968) (A.Y. Wong and K. Kondratenko).

PPG-100 "Current Sheets in Drift Waves in Plasmas", Phys. Fluids **11**, 274 (1968)(S.L. Ossakow and B.D. Fried).

PPG-101 "Resonant Stabilization of Electrons During Substorms", Phys. Fluids **12**, 1489 (1969)(C.S. Liu).

PPG-102 "Resonant Stabilization of Electrons During Substorms", Phys. Fluids **12**, 1489 (1969)(C.S. Liu).

PPG-103 "Resonant Stabilization of Electrons During Substorms", Phys. Fluids **12**, 1489 (1969)(C.S. Liu).

PPG-104 "Resonant Stabilization of Electrons During Substorms", Phys. Fluids **12**, 1489 (1969)(C.S. Liu).

PPG-105 "Resonant Stabilization of Electrons During Substorms", Phys. Fluids **12**, 1489 (1969)(C.S. Liu).

PPG-106 "Resonant Stabilization of Electrons During Substorms", Phys. Fluids **12**, 1489 (1969)(C.S. Liu).

PPG-107 "Resonant Stabilization of Electrons During Substorms", Phys. Fluids **12**, 1489 (1969)(C.S. Liu).

PPG-108 "Resonant Stabilization of Electrons During Substorms", Phys. Fluids **12**, 1489 (1969)(C.S. Liu).

PPG-109 "Resonant Stabilization of Electrons During Substorms", Phys. Fluids **12**, 1489 (1969)(C.S. Liu).

PPG-110 "Resonant Stabilization of Electrons During Substorms", Phys. Fluids **12**, 1489 (1969)(C.S. Liu).

PPG-111 "Non Heating via Turbulent Ion Acoustic Waves", Phys. Rev. Lett., **29**, 34 (1972)(K. Taylor and F.V. Coroniti).

PPG-112 "Polarization of the Auroral Electrojet", J. Geophys. Res., **77**, 2835 (1972)(F.V. Coroniti and C.F. Kennel).

PPG-113 "Cooperation and Wave Particle Interactions for Unstable Ion Acoustic Waves", Phys. Fluids **15**, 2275 (1972)(F.V. Coroniti and R.W. Holzer).

PPG-114 "Electrostatic Instability of Ring Currents Beyond the Plasmapause During Injection Events", J. Geophys. Res., **77**, 2835 (1972)(F.V. Coroniti and R.W. Holzer).

PPG-115 "Polarization of the Outer Planets", Space Sci. Rev., **14**, 51 (1973)(C.F. Kennel).

PPG-116 "Magnetospheric Transport and Longitudinal Heat Flow in a Laser-Based Magnetically Confined Arc Plasma", Phys. Rev. Lett., **26**, 424 (1971)(S.W. Fay, F. Chen, and D. E. Larson).

PPG-117 "Measurement of Transverse and Longitudinal Heat Flow in a Laser-Based Magnetically Confined Arc Plasma", Phys. Rev. Lett., **26**, 428 (1971)(S.W. Fay, F. Chen, and D. E. Larson).

PPG-118 "Large Oscillations, Quiescent Plasma in a Magnetospheric Shock Wave", J. Geophys. Res., **78**, 1581 (1973)(F.V. Coroniti and R.W. Holzer).

PPG-119 "Plasmaphysicist's Bias", J. Geophys. Res., **77**, 3608 (1972)(F.V. Coroniti and R.W. Thorne).

PPG-120 "Observation of Strong Ion-Acoustic Waves in an Inhomogeneous Vlasov Plasma", Dissertation, January (1970)(A.Y. Wong).

PPG-121 "Observation of Strong Ion-Acoustic Wave-Wave Interaction", January (1970)(A.Y. Wong and H. Isen).

PPG-122 "Effect of Toller-Pianka Collisions on Plasma Wave Echoes", Phys. Fluids **13**, 2348 (1970)(H. Isen and R.J. Taylor).

PPG-123 "Effect of Toller-Pianka Collisions on Ion Acoustic Harmonic Waves", Phys. Fluids **13**, 2374 (1970)(H. Isen and R.J. Taylor).

PPG-124 "The Analytic and Approximate Properties of the Plasma Dispersion Function", February (1970)(A. Banos and G. Johnston).

PPG-125 "Effect of Ion-Neutral Collisions and Ion Wave Turbulence on the Ion Wave Echo", June (1970)(D. Baker).

PPG-126 "Efficient Nonadiabatic Coupling Between Electron and Ion Resonances in Magnetoturbulent Plasmas", Phys. Rev. Lett., **25**, 1281 (1970)(A. Banos).

PPG-127 "Direct Measurements of Linear Growth Rates and Nonlinear Saturation Coefficients", Phys. Fluids **13**, 163 (1969).

PPG-128 "Electron Precipitation Pulses", J. Geophys. Res., **75**, 1263 (1970)(F. Coroniti and C.F. Kennel).

PPG-129 "Nonlinear Precipitation Instability", J. Geophys. Res., **75**, 1263 (1970)(F. Coroniti and C.F. Kennel).

PPG-130 "Linear and Nonlinear Coupling Between Ion and Wave Turbulence in the Ionosphere", Phys. Fluids **13**, 116 (1970)(G. Johnston).

PPG-131 "Observation of 1st order Ion Energy Distortion in Ion Acoustic Waves", Phys. Fluids **13**, 1281 (1970).

PPG-132 "Nonlinear Oscillatory Phenomena with Drift Waves in Plasmas", J. Applied Physics, **41**, 738 (1970)(H. Isen).

PPG-133 "Nonlinear Oscillatory Phenomena with Drift Waves in Plasmas", J. Geophys. Res., **75**, 1270 (1970)(H. Isen).

PPG-134 "Nonlinear Oscillatory Phenomena with Drift Waves in Plasmas", J. Geophys. Res., **75**, 1270 (1970)(F. Coroniti and C.F. Kennel).

PPG-135 "Nonlinear Oscillations in a Magnetoturbulent System", J. Geophys. Res., **75**, 1270 (1970)(F. Coroniti and C.F. Kennel).

PPG-136 "Effect of Toller-Pianka Collisions on Ion Acoustic Harmonic Waves", Phys. Fluids **13**, 2374 (1970)(H. Isen and R.J. Taylor).

PPG-137 "Resonance of Collisionless Electromagnetic Shocks", Phys. Fluids **13**, 2374 (1970)(H. Isen and R.J. Taylor).

PPG-138 "Resonance of Collisionless Electromagnetic Shocks", Phys. Fluids **13**, 2374 (1970)(H. Isen and R.J. Taylor).

PPG-139 "Resonance of Collisionless Electromagnetic Shocks", Phys. Fluids **13**, 2374 (1970)(H. Isen and R.J. Taylor).

PPG-140 "Resonance of Collisionless Electromagnetic Shocks", Phys. Fluids **13**, 2374 (1970)(H. Isen and R.J. Taylor).

PPG-141 "Resonance of Collisionless Electromagnetic Shocks", Phys. Fluids **13**, 2374 (1970)(H. Isen and R.J. Taylor).

PPG-142 "Resonance of Collisionless Electromagnetic Shocks", Phys. Fluids **13**, 2374 (1970)(H. Isen and R.J. Taylor).

PPG-143 "Resonance of Collisionless Electromagnetic Shocks", Phys. Fluids **13**, 2374 (1970)(H. Isen and R.J. Taylor).

PPG-144 "Resonance of Collisionless Electromagnetic Shocks", Phys. Fluids **13**, 2374 (1970)(H. Isen and R.J. Taylor).

PPG-145 "Resonance of Collisionless Electromagnetic Shocks", Phys. Fluids **13**, 2374 (1970)(H. Isen and R.J. Taylor).

PPG-146 "Resonance of Collisionless Electromagnetic Shocks", Phys. Fluids **13**, 2374 (1970)(H. Isen and R.J. Taylor).

PPG-147 "Resonance of Collisionless Electromagnetic Shocks", Phys. Fluids **13**, 2374 (1970)(H. Isen and R.J. Taylor).

PPG-148 "Resonance of Collisionless Electromagnetic Shocks", Phys. Fluids **13**, 2374 (1970)(H. Isen and R.J. Taylor).

PPG-149 "Resonance of Collisionless Electromagnetic Shocks", Phys. Fluids **13**, 2374 (1970)(H. Isen and R.J. Taylor).

PPG-150 "Resonance of Collisionless Electromagnetic Shocks", Phys. Fluids **13**, 2374 (1970)(H. Isen and R.J. Taylor).

PPG-151 "Resonance of Collisionless Electromagnetic Shocks", Phys. Fluids **13**, 2374 (1970)(H. Isen and R.J. Taylor).

PPG-152 "Resonance of Collisionless Electromagnetic Shocks", Phys. Fluids **13**, 2374 (1970)(H. Isen and R.J. Taylor).

PPG-153 "Resonance of Collisionless Electromagnetic Shocks", Phys. Fluids **13**, 2374 (1970)(H. Isen and R.J. Taylor).

PPG-154 "Resonance of Collisionless Electromagnetic Shocks", Phys. Fluids **13**, 2374 (1970)(H. Isen and R.J. Taylor).

PPG-155 "Resonance of Collisionless Electromagnetic Shocks", Phys. Fluids **13**, 2374 (1970)(H. Isen and R.J. Taylor).

PPG-156 "Resonance of Collisionless Electromagnetic Shocks", Phys. Fluids **13**, 2374 (1970)(H. Isen and R.J. Taylor).

PPG-157 "Resonance of Collisionless Electromagnetic Shocks", Phys. Fluids **13**, 2374 (1970)(H. Isen and R.J. Taylor).

PPG-158 "Resonance of Collisionless Electromagnetic Shocks", Phys. Fluids **13**, 2374 (1970)(H. Isen and R.J. Taylor).

PPG-159 "Resonance of Collisionless Electromagnetic Shocks", Phys. Fluids **13**, 2374 (1970)(H. Isen and R.J. Taylor).

PPG-160 "Resonance of Collisionless Electromagnetic Shocks", Phys. Fluids **13**, 2374 (1970)(H. Isen and R.J. Taylor).

PPG-161 "Resonance of Collisionless Electromagnetic Shocks", Phys. Fluids **13**, 2374 (1970)(H. Isen and R.J. Taylor).

PPG-162 "Resonance of Collisionless Electromagnetic Shocks", Phys. Fluids **13**, 2374 (1970)(H. Isen and R.J. Taylor).

PPG-163 "Resonance of Collisionless Electromagnetic Shocks", Phys. Fluids **13**, 2374 (1970)(H. Isen and R.J. Taylor).

PPG-164 "Resonance of Collisionless Electromagnetic Shocks", Phys. Fluids **13**, 2374 (1970)(H. Isen and R.J. Taylor).

PPG-165 "Resonance of Collisionless Electromagnetic Shocks", Phys. Fluids **13**, 2374 (1970)(H. Isen and R.J. Taylor).

PPG-166 "Resonance of Collisionless Electromagnetic Shocks", Phys. Fluids **13**, 2374 (1970)(H. Isen and R.J. Taylor).

PPG-167 "Resonance of Collisionless Electromagnetic Shocks", Phys. Fluids **13**, 2374 (1970)(H. Isen and R.J. Taylor).

PPG-168 "Resonance of Collisionless Electromagnetic Shocks", Phys. Fluids **13**, 2374 (1970)(H. Isen and R.J. Taylor).

PPG-169 "Resonance of Collisionless Electromagnetic Shocks", Phys. Fluids **13**, 2374 (1970)(H. Isen and R.J. Taylor).

PPG-170 "Resonance of Collisionless Electromagnetic Shocks", Phys. Fluids **13**, 2374 (1970)(H. Isen and R.J. Taylor).

PPG-171 "Resonance of Collisionless Electromagnetic Shocks", Phys. Fluids **13**, 2374 (1970)(H. Isen and R.J. Taylor).

PPG-172 "Resonance of Collisionless Electromagnetic Shocks", Phys. Fluids **13**, 2374 (1970)(H. Isen and R.J. Taylor).

PPG-173 "Resonance of Collisionless Electromagnetic Shocks", Phys. Fluids **13**, 2374 (1970)(H. Isen and R.J. Taylor).

PPG-174 "Resonance of Collisionless Electromagnetic Shocks", Phys. Fluids **13**, 2374 (1970)(H. Isen and R.J. Taylor).

PPG-175 "Resonance of Collisionless Electromagnetic Shocks", Phys. Fluids **13**, 2374 (1970)(H. Isen and R.J. Taylor).

PPG-176 "Resonance of Collisionless Electromagnetic Shocks", Phys. Fluids **13**, 2374 (1970)(H. Isen and R.J. Taylor).

PPG-177 "Resonance of Collisionless Electromagnetic Shocks", Phys. Fluids **13**, 2374 (1970)(H. Isen and R.J. Taylor).

PPG-178 "Resonance of Collisionless Electromagnetic Shocks", Phys. Fluids **13**, 2374 (1970)(H. Isen and R.J. Taylor).

PPG-179 "Resonance of Collisionless Electromagnetic Shocks", Phys. Fluids **13**, 2374 (1970)(H. Isen and R.J. Taylor).

PPG-180 "Resonance of Collisionless Electromagnetic Shocks", Phys. Fluids **13**, 2374 (1970)(H. Isen and R.J. Taylor).

PPG-181 "Resonance of Collisionless Electromagnetic Shocks", Phys. Fluids **13**, 2374 (1970)(H. Isen and R.J. Taylor).

PPG-182 "Resonance of Collisionless Electromagnetic Shocks", Phys. Fluids **13**, 2374 (1970)(H. Isen and R.J. Taylor).

PPG-183 "Resonance of Collisionless Electromagnetic Shocks", Phys. Fluids **13**, 2374 (1970)(H. Isen and R.J. Taylor).

PPG-184 "Resonance of Collisionless Electromagnetic Shocks", Phys. Fluids **13**, 2374 (1970)(H. Isen and R.J. Taylor).

PPG-185 "Resonance of Collisionless Electromagnetic Shocks", Phys. Fluids **13**, 2374 (1970)(H. Isen and R.J. Taylor).

PPG-186 "Resonance of Collisionless Electromagnetic Shocks", Phys. Fluids **13**, 2374 (1970)(H. Isen and R.J. Taylor).

PPG-187 "Resonance of Collisionless Electromagnetic Shocks", Phys. Fluids **13**, 2374 (1970)(H. Isen and R.J. Taylor).

PPG-188 "Resonance of Collisionless Electromagnetic Shocks", Phys. Fluids **13**, 2374 (1970)(H. Isen and R.J. Taylor).

PPG-189 "Resonance of Collisionless Electromagnetic Shocks", Phys. Fluids **13**, 2374 (1970)(H. Isen and R.J. Taylor).

PPG-190 "Resonance of Collisionless Electromagnetic Shocks", Phys. Fluids **13**, 2374 (1970)(H. Isen and R.J. Taylor).

PPG-191 "Resonance of Collisionless Electromagnetic Shocks", Phys. Fluids **13**, 2374 (1970)(H. Isen and R.J. Taylor).

PPG-192 "Resonance of Collisionless Electromagnetic Shocks", Phys. Fluids **13**, 2374 (1970)(H. Isen and R.J. Taylor).

PPG-193 "Resonance of Collisionless Electromagnetic Shocks", Phys. Fluids **13**, 2374 (1970)(H. Isen and R.J. Taylor).

PPG-194 "Resonance of Collisionless Electromagnetic Shocks", Phys. Fluids **13**, 2374 (1970)(H. Isen and R.J. Taylor).

PPG-195 "Resonance of Collisionless Electromagnetic Shocks", Phys. Fluids **13**, 2374 (1970)(H. Isen and R.J. Taylor).

PPG-196 "Resonance of Collisionless Electromagnetic Shocks", Phys. Fluids **13**, 2374 (1970)(H. Isen and R.J. Taylor).

PPG-197 "Resonance of Collisionless Electromagnetic Shocks", Phys. Fluids **13**, 2374 (1970)(H. Isen and R.J. Taylor).

PPG-198 "Resonance of Collisionless Electromagnetic Shocks", Phys. Fluids **13**, 2374 (1970)(H. Isen and R.J. Taylor).

PPG-199 "Resonance of Collisionless Electromagnetic Shocks", Phys. Fluids **13**, 2374 (1970)(H. Isen and R.J. Taylor).

PPG-200 "Resonance of Collisionless Electromagnetic Shocks", Phys. Fluids **13**, 2374 (1970)(H. Isen and R.J. Taylor).

PPG-201 "Resonance of Collisionless Electromagnetic Shocks", Phys. Fluids **13**, 2374 (1970)(H. Isen and R.J. Taylor).

PPG-202 "Resonance of Collisionless Electromagnetic Shocks", Phys. Fluids **13**, 2374 (1970)(H. Isen and R.J. Taylor).

PPG-203 "Resonance of Collisionless Electromagnetic Shocks", Phys. Fluids **13**, 2374 (1970)(H. Isen and R.J. Taylor).

PPG-204 "Resonance of Collisionless Electromagnetic Shocks", Phys. Fluids **13**, 2374 (1970)(H. Isen and R.J. Taylor).

PPG-205 "Resonance of Collisionless Electromagnetic Shocks", Phys. Fluids **13**, 2374 (1970)(H. Isen and R.J. Taylor).

PPG-206 "Resonance of Collisionless Electromagnetic Shocks", Phys. Fluids **13**, 2374 (1970)(H. Isen and R.J. Taylor).

PPG-207 "Resonance of Collisionless Electromagnetic Shocks", Phys. Fluids **13**, 2374 (1970)(H. Isen and R.J. Taylor).

PPG-208 "Resonance of Collisionless Electromagnetic Shocks", Phys. Fluids **13**, 2374 (1970)(H. Isen and R.J. Taylor).

PPG-209 "Resonance of Collisionless Electromagnetic Shocks", Phys. Fluids **13**, 2374 (1970)(H. Isen and R.J. Taylor).

PPG-210 "Resonance of Collisionless Electromagnetic Shocks", Phys. Fluids **13**, 2374 (1970)(H. Isen and R.J. Taylor).

PPG-211 "Resonance of Collisionless Electromagnetic Shocks", Phys. Fluids **13**, 2374 (1970)(H. Isen and R.J. Taylor).

PPG-212 "Resonance of Collisionless Electromagnetic Shocks", Phys. Fluids **13**, 2374 (1970)(H. Isen and R.J. Taylor).

PPG-213 "Resonance of Collisionless Electromagnetic Shocks", Phys. Fluids **13**, 2374 (1970)(H. Isen and R.J. Taylor).

PPG-214 "Resonance of Collisionless Electromagnetic Shocks", Phys. Fluids **13**, 2374 (1970)(H. Isen and R.J. Taylor).

PPG-215 "Resonance of Collisionless Electromagnetic Shocks", Phys. Fluids **13**, 2374 (1970)(H. Isen and R.J. Taylor).

PPG-216 "Resonance of Collisionless Electromagnetic Shocks", Phys. Fluids **13**, 2374 (1970)(H. Isen and R.J. Taylor).

PPG-217 "Resonance of Collisionless Electromagnetic Shocks", Phys. Fluids **13**, 2374 (1970)(H. Isen and R.J. Taylor).

PPG-218 "Resonance of Collisionless Electromagnetic Shocks", Phys. Fluids **13**, 2374 (1970)(H. Isen and R.J. Taylor).

PPG-219 "Resonance of Collisionless Electromagnetic Shocks", Phys. Fluids **13**, 2374 (1970)(H. Isen and R.J. Taylor).

PPG-220 "Resonance of Collisionless Electromagnetic Shocks", Phys. Fluids **13**, 2374 (1970)(H. Isen and R.J. Taylor).

PPG-221 "Resonance of Collisionless Electromagnetic Shocks", Phys. Fluids **13**, 2374 (1970)(H. Isen and R.J. Taylor).

PPG-222 "Resonance of Collisionless Electromagnetic Shocks", Phys. Fluids **13**, 2374 (1970)(H. Isen and R.J. Taylor).

PPG-223 "Resonance of Collisionless Electromagnetic Shocks", Phys. Fluids **13**, 2374 (1970)(H. Isen and R.J. Taylor).

PPG-224 "Resonance of Collisionless Electromagnetic Shocks", Phys. Fluids **13**, 2374 (1970)(H. Isen and R.J. Taylor).

PPG-225 "Resonance of Collisionless Electromagnetic Shocks", Phys. Fluids **13**, 2374 (1970)(H. Isen and R.J. Taylor).

PPG-226 "Resonance of Collisionless Electromagnetic Shocks", Phys. Fluids **13**, 2374 (1970)(H. Isen and R.J. Taylor).

PPG-227 "Resonance of Collisionless Electromagnetic Shocks", Phys. Fluids **13**, 2374 (1970)(H. Isen and R.J. Taylor).

PPG-228 "Resonance of Collisionless Electromagnetic Shocks", Phys. Fluids **13**, 2374 (1970)(H. Isen and R.J. Taylor).

PPG-229 "Resonance of Collisionless Electromagnetic Shocks", Phys. Fluids **13**, 2374 (1970)(H. Isen and R.J. Taylor).

PPG-230 "Resonance of Collisionless Electromagnetic Shocks", Phys. Fluids **13**, 2374 (1970)(H. Isen and R.J. Taylor).

PPG-231 "Resonance of Collisionless Electromagnetic Shocks", Phys. Fluids **13**, 2374 (1970)(H. Isen and R.J. Taylor).

PPG-232 "Resonance of Collisionless Electromagnetic Shocks", Phys. Fluids **13**, 2374 (1970)(H. Isen and R.J. Taylor).

PPG-233 "Resonance of Collisionless Electromagnetic Shocks", Phys. Fluids **13**, 2374 (1970)(H. Isen and R.J. Taylor).

PPG-234 "Resonance of Collisionless Electromagnetic Shocks", Phys. Fluids **13**, 2374 (1970)(H. Isen and R.J. Taylor).

PPG-235 "Resonance of Collisionless Electromagnetic Shocks", Phys. Fluids **13**, 2374 (1970)(H. Isen and R.J. Taylor).

PPG-236 "Resonance of Collisionless Electromagnetic Shocks", Phys. Fluids **13**, 2374 (1970)(H. Isen and R.J. Taylor).

PPG-237 "Resonance of Collisionless Electromagnetic Shocks", Phys. Fluids **13**, 2374 (1970)(H. Isen and R.J. Taylor).

PPG-238 "Resonance of Collisionless Electromagnetic Shocks", Phys. Fluids **13**, 2374 (1970)(H. Isen and R.J. Taylor).

PPG-239 "Resonance of Collisionless Electromagnetic Shocks", Phys. Fluids **13**, 2374 (1970)(H. Isen and R.J. Taylor).

PPG-240 "Resonance of Collisionless Electromagnetic Shocks", Phys. Fluids **13**, 2374 (1970)(H. Isen and R.J. Taylor).

PPG-241 "Resonance of Collisionless Electromagnetic Shocks", Phys. Fluids **13**, 2374 (1970)(H. Isen and R.J. Taylor).

PPG-242 "Resonance of Collisionless Electromagnetic Shocks", Phys. Fluids **13**, 2374 (1970)(H. Isen and R.J. Taylor).

PPG-243 "Resonance of Collisionless Electromagnetic Shocks", Phys. Fluids **13**, 2374 (1970)(H. Isen and R.J. Taylor).

PPG-244 "Resonance of Collisionless Electromagnetic Shocks", Phys. Fluids **13**, 2374 (1970)(H. Isen and R.J. Taylor).

PPG-245 "Resonance of Collisionless Electromagnetic Shocks", Phys. Fluids **13**, 2374 (1970)(H. Isen and R.J. Taylor).

PPG-246 "Resonance of Collisionless Electromagnetic Shocks", Phys. Fluids **13**, 2374 (1970)(H. Isen and R.J. Taylor).

PPG-247 "Resonance of Collisionless Electromagnetic Shocks", Phys. Fluids **13**, 2374 (1970)(H. Isen and R.J. Taylor).

PPG-248 "Resonance of Collisionless Electromagnetic Shocks", Phys. Fluids **13**, 2374 (1970)(H. Isen and R.J. Taylor).

PPG-249 "Resonance of Collisionless Electromagnetic Shocks", Phys. Fluids **13**, 2374 (1970)(H. Isen and R.J. Taylor).

PPG-250 "Resonance of Collisionless Electromagnetic Shocks", Phys. Fluids **13**, 2374 (1970)(H. Isen and R.J. Taylor).

PPG-251 "Resonance of Collisionless Electromagnetic Shocks", Phys. Fluids **13**, 2374 (1970)(H. Isen and R.J. Taylor).

PPG-252 "Resonance of Collisionless Electromagnetic Shocks", Phys. Fluids **13**, 2374 (1970)(H. Isen and R.J. Taylor).

PPG-253 "Resonance of Collisionless Electromagnetic Shocks", Phys. Fluids **13**, 2374 (1970)(H. Isen and R.J. Taylor).

PPG-254 "Resonance of Collisionless Electromagnetic Shocks", Phys. Fluids **13**, 2374 (1970)(H. Isen and R.J. Taylor).

PPG-255 "Resonance of Collisionless Electromagnetic Shocks", Phys. Fluids **13**, 2374 (1970)(H. Isen and R.J. Taylor).

PPG-256 "Resonance of Collisionless Electromagnetic Shocks", Phys. Fluids **13**, 2374 (1970)(H. Isen and R.J. Taylor).

PPG-257 "Resonance of Collisionless Electromagnetic Shocks", Phys. Fluids **13**, 2374 (1970)(H. Isen and R.J. Taylor).

PPG-258 "Resonance of Collisionless Electromagnetic Shocks", Phys. Fluids **13**, 2374 (1970)(H. Isen and R.J. Taylor).

PPG-259 "Resonance of Collisionless Electromagnetic Shocks", Phys. Fluids **13**, 2374 (1970)(H. Isen and R.J. Taylor).

PPG-260 "Resonance of Collisionless Electromagnetic Shocks", Phys. Fluids **13**, 2374 (1970)(H. Isen and R.J. Taylor).

PPG-261 "Resonance of Collisionless Electromagnetic Shocks", Phys. Fluids **13**, 2374 (1970)(H. Isen and R.J. Taylor).

PPG-262 "Resonance of Collisionless Electromagnetic Shocks", Phys. Fluids **13**, 2374 (1970)(H. Isen and R.J. Taylor).

PPG-263 "Resonance of Collisionless Electromagnetic Shocks", Phys. Fluids **13**, 2374 (1970)(H. Isen and R.J. Taylor).

PPG-264 "Resonance of Collisionless Electromagnetic Shocks", Phys. Fluids **13**, 2374 (1970)(H. Isen and R.J. Taylor).

PPG-265 "Resonance of Collisionless Electromagnetic Shocks", Phys. Fluids **13**, 2374 (1970)(H. Isen and R.J. Taylor).

PPG-266 "Resonance of Collisionless Electromagnetic Shocks", Phys. Fluids **13**, 2374 (1970)(H. Isen and R.J. Taylor).

PPG-267 "Resonance of Collisionless Electromagnetic Shocks", Phys. Fluids **13**, 2374 (1970)(H. Isen and R.J. Taylor).

PPG-268 "Resonance of Collisionless Electromagnetic Shocks", Phys. Fluids **13**, 2374 (1970)(H. Isen and R.J. Taylor).

PPG-269 "Resonance of Collisionless Electromagnetic Shocks", Phys. Fluids **13**, 2374 (1970)(H. Isen and R.J. Taylor).

PPG-270 "Resonance of Collisionless Electromagnetic Shocks", Phys. Fluids **13**, 2374 (1970)(H. Isen and R.J. Taylor).

PPG-271 "Resonance of Collisionless Electromagnetic Shocks", Phys. Fluids **13**, 2374 (1970)(H. Isen and R.J. Taylor).

PPG-272 "Resonance of Collisionless Electromagnetic Shocks", Phys. Fluids **13**, 2374 (1970)(H. Isen and R.J. Taylor).

PPG-273 "Resonance of Collisionless Electromagnetic Shocks", Phys. Fluids **13**, 2374 (1970)(H. Isen and R.J. Taylor).

PPG-274 "Resonance of Collisionless Electromagnetic Shocks", Phys. Fluids **13**, 2374 (1970)(H. Isen and R.J. Taylor).

PPG-275 "Resonance of Collisionless Electromagnetic Shocks", Phys. Fluids **13**, 2374 (1970)(H. Isen and R.J. Taylor).

PPG-276 "Resonance of Collisionless Electromagnetic Shocks", Phys. Fluids **13**, 2374 (1970)(H. Isen and R.J. Taylor).

PPG-277 "Resonance of Collisionless Electromagnetic Shocks", Phys. Fluids **13**, 2374 (1970)(H. Isen and R.J. Taylor).

PPG-278 "Resonance of Collisionless Electromagnetic Shocks", Phys. Fluids **13**, 2374 (1970)(H. Isen and R.J. Taylor).

PPG-279 "Resonance of Collisionless Electromagnetic Shocks", Phys. Fluids **13**, 2374 (1970)(H. Isen and R.J. Taylor).

PPG-280 "Resonance of Collisionless Electromagnetic Shocks", Phys. Fluids **13**, 2374 (1970)(H. Isen and R.J. Taylor).

PPG-281 "Resonance of Collisionless Electromagnetic Shocks", Phys. Fluids **13**, 2374 (1970)(H. Isen and R.J. Taylor).

PPG-282 "Resonance of Collisionless Electromagnetic Shocks", Phys. Fluids **13**, 2374 (1970)(H. Isen and R.J. Taylor).

PPG-283 "Resonance of Collisionless Electromagnetic Shocks", Phys. Fluids **13**, 2374 (1970)(H. Isen and R.J. Taylor).

PPG-284 "Resonance of Collisionless Electromagnetic Shocks", Phys. Fluids **13**, 2374 (1970)(H. Isen and R.J. Taylor).

PPG-285 "Resonance of Collisionless Electromagnetic Shocks", Phys. Fluids **13**, 2374 (1970)(H. Isen and R.J. Taylor).

PPG-286 "Resonance of Collisionless Electromagnetic Shocks", Phys. Fluids **13**, 2374 (1970)(H. Isen and R.J. Taylor).

PPG-287 "Resonance of Collisionless Electromagnetic Shocks", Phys. Fluids **13**, 2374 (1970)(H. Isen and R.J. Taylor).

PPG-288 "Resonance of Collisionless Electromagnetic Shocks", Phys. Fluids **13**, 2374 (1970)(H. Isen and R.J. Taylor).

PPG-289 "Resonance of Collisionless Electromagnetic Shocks", Phys. Fluids **13**, 2374 (1970)(H. Isen and R.J. Taylor).

PPG-290 "Resonance of Collisionless Electromagnetic Shocks", Phys. Fluids **13**, 2374 (1970)(H. Isen and R.J. Taylor).

PPG-291 "Resonance of Collisionless Electromagnetic Shocks", Phys. Fluids **1**

- PPC-124** "Calculation of Reflection and Transmission Coefficients for a Class of One-Dimensional Wave Propagation Problems in Inhomogeneous Media", J. Math. Phys. **15**, 943 (1973)(A. Rabinovitz).
- PPC-125 "One-Dimensional wave Functions for Particular Plasma Density Profiles", Phys. Fluids **17**, 2275 (1974)(A. Rabinovitz and B. White).
- PPC-126 "Nonlinear Ion-Electromagnetic Waves in One-dimensional Plasmas", J. Plasma Phys. **16**, 527 (1974)(F. Chen and B. White).
- PPC-127 "Instabilities produced by Nonlinear Electromagnetic Waves in One-dimensional Plasmas", Phys. Soc. Div. of Plasma Physics Annual Meeting, November 13-16 (1972).
- PPC-128 "Nonlinear Instabilities produced by Nonlinear Electromagnetic Convection", J. Plasma Phys. **16**, 2037 (1972)(F. V. Coroniti and C.F. Kennel).
- PPC-129 "Nonlinear Stabilization of Oscillating Two-Stream Instability", Phys. Fluids **16**, 1380 (1973)(K. Nishikawa, Y.C. Lee and P.K. Shukla).
- PPC-130 "Oscillations in Finite Beta Plasmas", Dissertation October (1972)(M.S. Chen).
- PPC-131 "Wave Packet Formation of Nonlinear Plasma Wave Statistics", Phys. Fluids **16**, 1331 (1973)(K. Nishikawa, Y.C. Lee and B.D. Fried).
- PPC-132 "Resonant Excitation of Electrostatic Waves with Electromagnetic Waves", Phys. Fluids **16**, 1376 (1973)(G. Schmitz).
- PPC-133 "Resonant Ion Source and Free-Stream Beam Diagnostic Techniques", Rev. Sci. Instrum. **46**, 617 (1973)(R.L. Stenzel).
- PPC-134 "Electron Plasma Waves in an Unbounded Uniform Magnetoplasma", Phys. Fluids **16**, 545 (1973)(R.L. Stenzel).
- PPC-135 "Convergent Amplification in the Equatorial Electrojet", J. Geophys. Res. **78**, 4619 (1973)(K. Lee).
- PPC-136 "Effects of Projection Parallel to the Magnetic Field on the Type I Electrojet Irregularity Instability", Planetary and Space Sci. **21**, 1339 (1973)(J.-I. Lee and C.F. Kennel).
- PPC-137 "Scaling Computer Simulation of Parametric Instabilities", November (1972)(R.L. Stenzel).
- PPC-138 "Theory of Nonlocal Resonance Parametric Excitation in Plasmas", Phys. Fluids **16**, 2270 (1973)(D. Arnush, B.D. Fried, C. Kennel, A. Nishikawa and A.Y. Wong).
- PPC-139 "Stability and Trapping of Electromagnetic Radiation in Plasmas", Phys. Fluids **16**, 1522 (1973)(P. Kaw, G. Schmidt and T. Milicos).
- PPC-140 "Finite Beta Drift Instability", J. Geophys. Res. **78**, 2121 (1973)(K. S. Liu, H. Chen and K. Nishikawa).
- PPC-141 "The Variation of Ion Acoustic Shocklets", Phys. Fluids **16**, 2157 (1973)(A.Y. Wong).
- PPC-142 "Experiments on Parametric Instabilities", March (1973)(A.Y. Wong).
- PPC-143 "On the Marginal Stability Saturation Spectrum of Instable Type I (Equatorial Electrojet Irregularities)", J. Geophys. Res., **78**, 1364 (1973)(C.F. Kennel, G. Schmidt and T. Milicos).
- PPC-144 "Relativistic Particle Motion in Nonuniform Electromagnetic Waves", Phys. Fluids **16**, 1380 (1973)(G. Schmidt and C. Schmitz).
- PPC-145 "Evolution of Kink Like Modes with Trapped Electrons", Phys. Rev. Lett. **30**, 1299 (1973)(Y. Wong, B.H. Quon and C.F. Kennel).
- PPC-146 "Stabilization of Ion Acoustic Waves by Electron Trapping", Phys. Fluids **16**, 206 (1973)(M. Ahnert).
- PPC-147 "Turbulence in Electrostatic Ion Acoustic Shock", Phys. Fluids **16**, 2804 (1973)(M. M. Meissner, F.V. Coroniti, A.Y. Wong and B. White).
- PPC-148 "Theory of Dielectric Function in Pulseless", Phys. Rev. Lett. **31**, 1384 (1973)(C.F. Kennel).
- PPC-149 "Physical Interpretation of the Oscillatory Line-Spectrum", June (1973)(C.F. Lee and C.S. Liu).
- PPC-150 "Relativistic Particle Motion in Nonuniform Electromagnetic Waves", Phys. Rev. Lett. **31**, 1380 (1973)(G. Schmidt and C. Schmitz).
- PPC-151 "Kinetic Current and Magnetic Storms", Radio Sci., **8**, 1007 (1973)(F.V. Coroniti).
- PPC-152 "Stably Trapped Proton Fluxes in the Jovian Magnetosphere", Astrophys. J., **195**, 395 (1974)(F.V. Coroniti, C.F. Kennel and B. D. Fried).
- PPC-153 "Relativistic Raman Scattering Instabilities in an inhomogeneous Plasma", Phys. Rev. Lett. **21**, 1197 (1973)(J.F. Drake and Y.C. Lee).
- PPC-154 "Growth and Saturation of the Absolute Electron Cyclotron Drift Instability", Phys. Fluids **17**, 778 (1974)(J.F. Drake and Y.C. Lee).
- PPC-155 "Nonlinear Instabilities of Electrically Charged Particles in Plasmas", J. Plasma Phys. **10**, 1545 (1973)(R.L. Stenzel and B.H. Quon).
- PPC-156 "Nonlinear Instabilities of Electrically Charged Particles in Plasmas", Congress on Waves and Instabilities in Plasmas, Innsbruck, Austria (Y.C. Lee).
- PPC-157 "Parametric Instabilities of Electrically Charged Particles in Plasmas", J. Plasma Phys. **10**, 1546 (1973)(R.L. Stenzel and B.H. Quon).
- PPC-158 "Parametric Instabilities of Electromagnetic Waves in Plasmas", Phys. Fluids **16**, 2279 (1973)(F. V. Coroniti).
- PPC-159 "Nonlinear Optics of Plasmas", Survey Lecture of Int'l. Congress on Waves and Instabilities in Plasmas, Innsbruck, Austria (Y.C. Lee).
- PPC-160 "Physical Mechanisms for Laser and Plasma Near-Resonant Parametric Instabilities", J. Plasma Phys. **10**, 155 (1973)(F. V. Coroniti).
- PPC-161 "Mechanisms of Laser and Plasma Near-Resonant Parametric Instabilities", J. Plasma Phys. **10**, 155 (1973)(F. V. Coroniti).
- PPC-162 "Abstracted Review", Int'l. Congress on Waves and Instabilities in Plasmas, Innsbruck, Austria (Y.C. Lee and J.M. Dawson).
- PPC-163 "Abstracted Review", Int'l. Congress on Waves and Instabilities in Plasmas, Innsbruck, Austria (Y.C. Lee and J.M. Dawson).
- PPC-164 "Relativistic Nonlinear Schrödinger's Equation Model of Oscillating Two-Stream Instability", Phys. Rev. Lett. **22**, 457 (1974)(G. Morales).
- PPC-165 "Nonresonant Scattering Processes in Electron Beam-Plasma Interaction including Ion Dynamics", Phys. Rev. Lett. **22**, 466 (1974)(Y.C. Lee and B.H. White).
- PPC-166 "Nonresonant Scattering Processes in Electron Beam-Plasma Interaction including Ion Dynamics", Phys. Rev. Lett. **22**, 654 (1974).
- PPC-167 "Parametric Instabilities of Electromagnetic Waves in Inhomogeneous Plasmas", Phys. Rev. Lett. **22**, 654 (1974).
- PPC-168 "Langmuir Wave Turbulence - Condensation and Collapse", Com. Plasma Phys. and Cont. Plasma Phys. **1**, 111 (1970)(R.C. Lee, C.S. Liu and K. Nishikawa).
- PPC-169 "Consequences of Microplasmas on Geomagnetically Trapped Particles", Rev. Space Sci. **15**, 443 (1974)(R.M. Thorne).
- PPC-170 "Linear Wave Conversion in Inhomogeneous Plasmas", March (1974)(D.L. Kelly and A. Hanos).
- PPC-171 "The Cause of Solar-Affected Effects in the Middle Latitude D-Ring Ionosphere", J. Atmosphera and Terrestrial Phys. **19**, 223 (1974)(W.N. Syndercock and M. Thorndieke).
- PPC-172 "Application of an Electromagnetic Particle Simulation Code to the Generation of Electromagnetic Radiation", Phys. Fluids **16**, 234 (1973)(R.J. Stenzel).
- PPC-173 "The Coulombic Force Exited on a Plasma by an Infrared Laser Beam", Dissertation, March (1974)(M. Martic).
- PPC-174 "Comments on Two-Spectrum and Space Sci.", **16**, 71 (1975)(C.K. Stenzel and R. Stenzel).
- PPC-175 "Observation of the Ponderomotive Force and Acceleration on Non-uniform Plasma", Phys. Rev. Lett. **24** (1974)(C.K. Stenzel and A.Y. Wong).
- PPC-176 "Electron Beam-Plasma Interaction Including Ion Dynamics", Dissertation, June (1974)(B.H. Quon).
- PPC-177 "Linear Conversion and Parametric Instabilities in a Non-Uniform Plasma", Dissertation, June (1974)(H.C. Kim, R. Stenzel and A.Y. Wong).
- PPC-178 "Stimulated Compton Scattering of Electromagnetic Waves in Plasma", Phys. Fluids **18**, 201 (1975)(T. Lin and J.M. Dawson).
- PPC-179 "Inertialized Currents in a Collisional Plasma", Dissertation, July (1974)(M.K. Hudson).
- PPC-180 "Effect of the Ponderomotive Force in the Interaction of a Capacitor RF Field with a Nonuniform Plasma", Phys. Rev. Lett. **23**, 1016 (1974)(G.J. Morales and Y.C. Lee).
- PPC-181 "Quadrature of Ionospheric Tidal Winds by Uyeda Simulation", August (1974)(J.P. Scheidegger and S. Yamamoto).
- PPC-182 "Response of the Middle Latitude D-Region to Geomagnetic Storm", J. Atmos. and Terres. Phys. **19**(1974)(W. Spolyai).
- PPC-183 "Production of Negative Ions and Generation of Inverse Neutral Beams", Applied Phys. Lett. **25**, 379 (1974)(A.Y. Wong, J.M. Dawson and W. Gekelman).

- PPG-246 "Parametric Instabilities with Finite Wavelength Pump", Physics of Fluids, 19, 1975 (1976), (B. D. Fried, T. Ikemura, K. Nishikawa, and G. Schmidt.)
- PPG-247 "The Scattering of Cosmic Rays by Magnetic Bubbles", Astrophys. J., 205, 135 (1976), (R.F. Flewelling & F. V. Coroniti).
- PPG-248 "Plasma Simulation on the CHI Microprocessor System", (1975)(T. Kamimura, J.M. Dawson, B. Rosen, G.J. Culier, R.D. Levee and G. Ball).
- PPG-249 "Nonlinear Interactions of Focused Resonance Cone Fields with Plasmas", (1975)(R. Stenzel and W. Gekelman).
- PPG-250 "The Effect of Pump Cutoff on Parametric Instabilities in an Inhomogeneous Plasma", (1976)(J. VanDam and Y.C. Lee).
- PPG-251 "Parametric Excitation of Ion Density Fluctuations in the Relativistic Beam-Plasma Interaction", 19, 849(1976)Phys. Fluids (H. Schamel, Y.C. Lee and G.J. Morales).
- PPG-252 "The Spiky Turbulence Generated by a Propagating Electrostatic Wave of Finite Spatial Extent", Phys. Fluids 19, 690 (1976)
- (1976) (G.J. Morales and Y.C. Lee).
- PPG-253 "Departures from Theory of the Experimental Line Profile of Helium I 4471.5Å", January (1976)(J. Turecek).
- PPG-254 "Maintenance of the Middle Latitude Nocturnal D-Layer by Energetic Electron Precipitation", January (1976)(W. Spjeldvik and R. Thorne).
- PPG-255 "Free Boundaries for Plasmas in Surface Magnetic Field Configurations", Physics of Fluids, 19, 1909 (1976) (B. D. Fried, J. W. VanDam and Y. C. Lee).
- PPG-256 "Soliton-Like Structures in Plasmas", March (1976)(Y.C. Lee and G.J. Morales).
- PPG-257 "Magnetic Field Reconnection in a Collisionless Plasma", submitted to Astrophys. J. (1976)(F.V. Coroniti and A. Eviatar).
- PPG-258 "The Earth's Magnetosphere", accepted by Encyc. of Phys. (1976) (F.V. Coroniti).
- PPG-259 "Lossy Radial Diffusion of Relativistic Jovian Electrons", J.Geophys.Res.81, 4553 (1976) (D.D. Barbosa and F.V. Coroniti).
- PPG-260 "Relativistic Electrons and Whistlers in Jupiter's Magnetosphere", J.Geophys.Res., 81, 4531 (1976) (D.D. Barbosa and F.V. Coroniti).
- PPG-261 "A Self-Consistent Magnetostatic Particle Code for Numerical Simulation of Plasmas", submitted to J. Comp. Phys. (1976) (J. Busnardo-Neto, P.L. Pritchett, A.T. Lin and J.M. Dawson).
- PPG-262 "Relativistic Effects in Resonance Absorption", Physics of Fluids 19, 1772 (1976)(J.F. Drake and Y.C. Lee).
- PPG-263 "Convective Electron Loss Cone Instabilities", (M. Ashour-Abdalla and C. F. Kennel)
- PPG-264 "Experiments on Parametric Instabilities in Laser-Beam Plasma Interactions", F. Chen. Presented at Nobel Symposium.
- PPG-265 "The Local Time Variation of ELF Emissions During Periods of Substorm Activity", R. M. Thorne, F. R. Church, W. J. Malloy, B. T. Tsurutani, Submitted to Jrnal. of Geophys., July 1976.
- PPG-266 "An Investigation of Relativistic Electron Precipitation Events & Their Association with Magnetospheric Substorm Activity R. M. Thorne & T. R. Larsen, July 1976.
- PPG-267 "The Free Electron Laser", T. Kwan, J. M. Dawson, & A. T. Lin, Submitted to Phys. of Fluids, July 1976.
- PPG-268 "Stimulated Compton Scattering of Electromagnetic Waves Off Plasma Ions", A. T. Lin & J. M. Dawson, Submitted to Physics of Fluids, July 1976.
- PPG-269 "Stability of Shell Distributions", D. D. Barbosa, July 1976. Submitted to Planetary & Space Science.
- PPG-270 "Synchro-Compton Radiation Damping of Relativistically Strong Plasma Waves", C. F. Kennel, E. Asseo and R. Pellat, July 1976, Submitted to Science.
- PPG-271 "Particle and Wave Dynamics in a Magnetized Plasma Subject to High RF Pressure", W. Gekelman & R. L. Stenzel, July 1976, Submitted to Phys. Fluids.
- PPG-272 "Energetic Radiation Belt Electron Precipitation; A Natural Depletion Mechanism for Stratospheric Ozone", R. M. Thorne, July 1976, Submitted to Science.
- PPG-273 "CTR Using the P-11B Reaction", J. M. Dawson, August 1976.
- PPG-274 "San Francisco Abstracts-Papers to be Presented at San Francisco Meeting of the American Physical Society Division of Plasma Physics, November 15-19, 1976".

- PPG-275 "Surface Multipole Guide Field for Plasma Injection", R. A. Breun, B. H. Rael, & A. Y. Wong, Review of Scientific Instruments, Submitted September 1976.
- PPG-276 "Higher Order Adiabatic Invariants and Non-Adiabatic Diffusion for Geometric Mirrors", Y. C. Lee, T. K. Samec, & B. D. Fried, Phys. Fluids, Submitted July 1976.
- PPG-277 "Electromagnetic Interactions with Inhomogeneous Plasmas", A. Y. Wong.
- PPG-278 "The Importance of Electrostatic Ion-Cyclotron Instability for Quiet-Time Proton Auroral Precipitation", M. Ashour-Abdalla & R. M. Thorne, Geophys. Res. Lett., Submitted October 1976.
- PPG-679 "Self Channelling of Whistler Waves", E. S. Weibel, Phys. Rev. Lett., Submitted October 1976.
- PPG-280 "Formation of Potential Double Layers in Plasmas", B. H. Quon & A. Y. Wong, Phys. Rev. Lett., Submitted October 1976.
- PPG-281 "Plasma Confinement by Simple Magnetic Fields", T. K. Samec.
- PPG-282 "Kinetic Theory of Tearing Instabilities", J. F. Drake & Y. C. Lee.
- PPG-283 "Jupiter's Magnetosphere", C. F. Kennel & F. V. Coroniti, Annual Rev. of Astro. & Astrophys., Submitted November 1976.
- PPG-284 "Direct Density Display with a Resonance Cone RF Probe", J. Ickovic, R. L. Stenzel & W. Gekelman, Submitted to Rev. of Scientific Instr. as a Research Note.
- PPG-285 "The Ponderomotive Effect in a Magnetized Plasma", E. S. Weibel, Submitted to Phys. Fluids.
- PPG-286 "The Fluid Theory of the Ponderomotive Effect in a Magnetized Plasma", E. S. Weibel.
- PPG-287 "Possible Origins of Time Variability in Jupiter's Outer Magnetosphere", F. V. Coroniti & C. F. Kennel.
- PPG-288 "Coupling of Lower-Hybrid Radiation at the Plasma Edge", G. J. Morales, Phys. Fluids, Submitted January 1977.
- PPG-289 "Nonlinear Evolution of Collisionless and Semi-Collisional Tearing Modes", J. F. Drake and Y. C. Lee, Phys. Rev. Lett., Submitted January 1977.
- PPG-290 "Model Analysis for Shear Stabilization of Collisionless Drift Waves", Y. C. Lee & T. Tange.
- PPG-291 "Particle Orbits and Loss Regions in UCLA Tokamaks", C. P. Lee.
- PPG-292 "Generation of Density Cavities and Localized Electric Fields in a Nonuniform Plasma", G. J. Morales & Y. C. Lee, Phys. Fluids, Submitted January 1977.